THE THERMODEGRADATION AND THE DEGRADATION PRODUCTS OF POLYANILINE

By

TSUNG-CHIEH TSAI

Bachelor of Science

National Taiwan Institute of Technology

Taipei, Taiwan

1989

Submitted to the Faculty of the
Graduate College of the
Oklahoma State University
in partial fulfillment of
the requirements for
the Degree of
MASTER OF SCIENCE
July, 1992

THE THERMODEGRADATION AND THE

DEGRADATION PRODUCTS OF

POLYANILINE

Thesis Approved:

Alan Sue

Thesis Adviser

Robert K. Lewson Jr

Arland H. Johannes

Thomas C. Collins

Dean of the Graduate College

ACKNOWLEDGMENTS

I wish to express my sincere gratitude to my major advisor, Dr. David A. Tree, for his guidance, encouragement, interest and valuable suggestions. Gratitude is also extended to the other committee members, Drs. Robert L. Robinson, Jr., and Arland H. Johannes.

Special thanks are due to Oklahoma State University, School of Chemical Engineering, and University Center for Energy Research for the financial support I received during this research.

Finally, I would like to express my gratitude to my parents, Chao-chan Tsai and Chin-ying Tsai-Hu, and my lovely fiancee, Yann-jen Tarng, for many sacrifices, continuous support, much understanding and love, and never-ending patience throughout the course of this endeavor.

TABLE OF CONTENTS

Chapter — Page

I. INTRODUCTION 1

II. LITERATURE REVIEW 3

- Polyaniline structure 3
- Possible application 5
- Polyaniline synthesis method 7
- Polyaniline stability 8
- Kinetic parameters 14

III. EQUIPMENT, MATERIALS, AND PROCEDURES 21

- Thermogravimetric analysis 21
- Gas chromatograph 26
- Material preparation procedure 30

IV. RESULTS AND DISCUSSION 34

V. RECOMMENDATIONS AND CONCLUSIONS 63

BIBLIOGRAPHY 65

APPENDIXES

APPENDIX A - RAW DATA 68

APPENDIX B - DISCUSSION OF HIGHER REACTION ORDER . 81

APPENDIX C - COMPUTER PROGRAM 85

APPENDIX D - DSC DATA 92

APPENDIX E - SAMPLES OF GAS CHROMATOGRAM 95

LIST OF TABLES

Table		Page
I.	Visual Colors of Polyaniline Prepared at Various pH And Potential Values	6
II.	Some Typical Forms of g(W) and $-\int_{W_o}^{W} \frac{dW}{g(W)}$	20
III.	Examples of Parameter Settings for Micricon 823	24
IV.	Examples of Parameter Settings for Notebook	25
V.	Retention Times for the Components Analyzed	29
VI.	Kinetic Parameters of the Decomposition of Polyethylene	38
VII.	Kinetic Parameters of the Decomposition of Emeraldine Base	45
VIII.	Kinetic Parameters of the Decomposition of Sulfonated Emeraldine	52
IX.	Thermodegradation Products of Emeraldine Base	59
X.	Thermodegradation Products of Sulfonated Emeraldine	59

LIST OF FIGURES

Figure		Page
1.	Oxidative Degradation of Polyaniline in Aqueous Electrolyte	10
2.	Chlorination of Aromatic Ring in Polyaniline	12
3.	Backbone Decomposition Reaction of Polyaniline	15
4.	Experimental Setup	22
5.	Gas Chromatograph	27
6.	TGA Curves of Polyethylene at Various Heating Rates	35
7.	Thermogravimetric Curves of Polyethylene as a Function of the Reciprocal Absolute Temperature	36
8.	Plots of Logarithmic Heating Rate Against the Reciprocal Absolute Temperature for Different Decomposition Conversions of Polyethylene	37
9.	Comparison of the Calculated Curve with Different Reaction Order for Polyethylene	38
10.	Comparison of Experimental and Calculated TGA Curves of Polyethylene	41
11.	TGA Curves of Emeraldine Base at Various Heating Rate	42
12.	Plots of Logarithmic Heating Rate Against the Reciprocal Absolute Temperature for Different Decomposition Conversions of Emeraldine Base	43
13.	Comparison of the Calculated Curve with Different Reaction Orders for Emeraldine Base	44
14.	Comparison of Experimental and Calculated TGA Curves of Emeraldine Base at a Heating Rate of 3°C/min	46
15.	Doyle's Integral Term	48

Figure Page

16. Comparison of Experimental and Calculated TGA Curves of Emeraldine Base 49

17. TGA Curves of Sulfonated Emeraldine at Various Heating Rates Rate 1°C/min 50

18. Plots of Logarithmic Heating Rate Against the Reciprocal Absolute Temperature For Different Decomposition Conversions of Sulfonated Emeraldine 51

19. Comparison of Experimental and Calculated TGA Curve of Sulfonated Emeraldine 54

20. TGA Curve of Degradation Products Concentration of Emeraldine Base at a Constant Heating Rate 6.67°C/min in Helium Environment 57

21. TGA Curve and Degradation Products Concentration of Sulfonated Emeraldine at a Constant Heating Rate 6.67°C/min in Helium Environment 58

22. The Pyrolysis Products of Polyacrylonitrile and Proposed Pyrolysis Products of Polyaniline . . 61

23. TGA Curves of Polyethylene at a Constant Heating Rate 1°C/min 69

24. TGA Curves of Polyethylene at a Constant Heating Rate 3°C/min 70

25. TGA Curves of Polyethylene at a Constant Heating Rate 5°C/min 71

26. TGA Curves of Polyethylene at a Constant Heating Rate 10°C/min 72

27. TGA Curve of Emeraldine Base at a Constant Heating Rate 1°C/min 73

28. TGA Curve of Emeraldine Base at a Constant Heating Rate 3°C/min 74

29. TGA Curve of Emeraldine Base at a Constant Heating Rate 5°C/min 75

30. TGA Curve of Emeraldine Base at a Constant Heating Rate 10°C/min 76

31. TGA Curve of Sulfonated Emeraldine at a Constant Heating Rate 3°C/min 77

Figure Page

32. TGA Curve of Sulfonated Emeraldine at a Constant Heating Rate 5°C/min 78

33. TGA Curve of Sulfonated Emeraldine at a Constant Heating Rate 10°C/min 79

34. TGA Curve of Sulfonated Emeraldine at a Constant Heating Rate 15°C/min 80

35. DSC Curve of Emeraldine Base at Scanning Rate 10°C/min in Nitrogen Environment 93

36. DSC Curve of Sulfonated Emeraldine at Scanning Rate 10°C/min in Nitrogen Environment 94

37. Gas Chromatogram Peaks Order of Appearance 96

38. Gas Chromatogram Taken Before Degradation Began . . 97

39. Gas Chromatogram Taken at 716°C 97

40. Gas Chromatogram Taken 20 min After the Temperature Reached 925°C 98

LIST OF SYMBOLS

Symbol	
a	Heating rate; °C/min
A	The pre-exponential factor, the apparent frequency factor; min^{-1}
C_A	Concentration of component A; mole/liter
n	The order of the reaction
r_A	Rate of reaction of component A; mole/liter*min
R	The ideal gas constant; cal/mole*K
t	Time; min
t_0	Initial time; min
T	The absolute temperature; K
W	The fractional residual weight of the sample
W_0	The fractional residual weight of the sample at time t_0
ΔE	The apparent activation energy; kcal/mole

CHAPTER I

INTRODUCTION

Polymers that conduct electricity appear promising for a wide variety of uses, ranging from easily fabricated semiconductor chips and integrated circuits to electrodes, light weight battery components, sensors, electrochromic displays, and static-free packaging materials (1-13). Following the successful synthesis of polyacetylene (PAc), and its subsequent doping to a conducting form (14), the first widely recognized intrinsic electronically conducting polymer, has aroused great interest.

Many significant achievements, such as a prototype light weight rechargeable battery, have been reached by polyacetylene. However, problems still remain with the environmental stability, which requires polyacetylene to be in an inert atmosphere to prevent spontaneous combustion. In addition, PAc must be doped with a highly toxic substance.

The most promising, environmentally stable, conducting polymer material appears to be polyaniline (PA) which, in addition, doped with a non-toxic agent. The discovery of this material has lead to the development of a prototype rechargeable battery which is easily manufactured, relatively inexpensive, light weight, and non-toxic. These

features allow the PA to compete with the conventional, heavy, expensive, toxic, and hazardous lead acid battery.

The purpose of this research was to define the thermodegradation behavior by thermogravimetric analysis (TGA) and gas chromatography (GC) to determine the kinetic parameters and degradation products. This work has significant implications for future uses of PA because the chain scission of PA can be predicted, and the anti-degradation additives can be further investigated based on this study.

CHAPTER II

LITERATURE REVIEW

This chapter discusses the structure of polyaniline, the potential applications, the synthesis method, the thermostability, the degradation products and the data analysis method for the thermogravimetric analysis (TGA) technique.

Polyaniline Structure

Polyanilines were synthesized as early as 1910 by Green and Woodhead (15). However, little interest was shown in this material until it was "rediscovered" by MacDiarmid in 1984 who proposed the nomenclature used throughout this thesis (1). Polyaniline base has the general formula

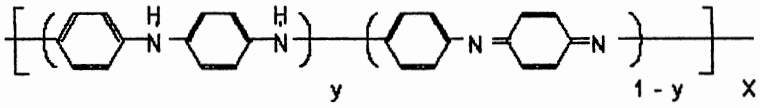

(II. 1)

where y indicates the number of "reduced" mers, and 1-y gives the number of oxidized mers. The value of y can vary from 1 (fully reduced polyaniline called leucoemeraldine):

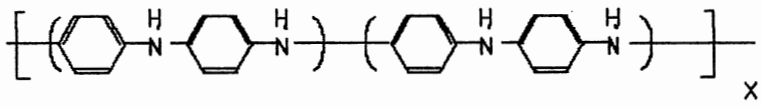

(II. 2)

to 0 (fully oxidized polyaniline called pernigraniline):

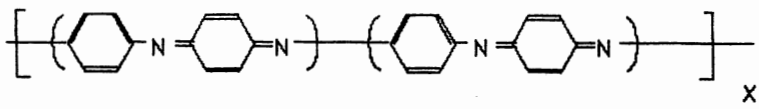

(II. 3)

Emeraldine base (y = 0.5) consists of alternating oxidized and reduced repeat units, and has a conductivity at room temperature of 10^{-10} S/cm (16).

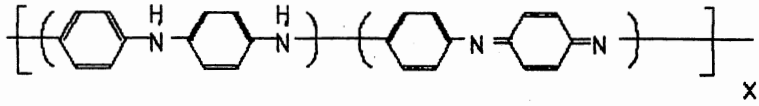

(II. 4)

The imine nitrogen atoms of the polymeric base can be doped in whole or in part to give the corresponding salt. Emeraldine base can be completely doped externally by hydrochloric acid to the metallic region yielding emeraldine hydrochloride:

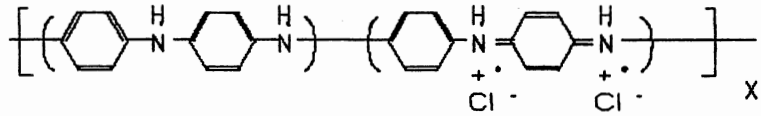

(II. 5)

or

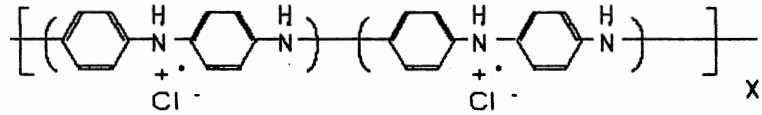

; (II. 6)

or internally substituted by sulfonic acid, to produce sulfonated emeraldine:

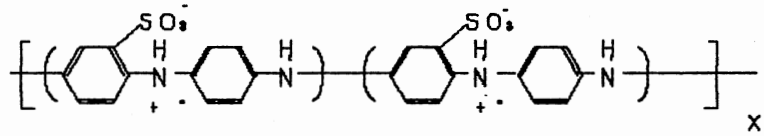

(II. 7)

The conductivity of the polymeric base depends on the

oxidation state and on the Ph of the aqueous acid. The conductivity of polyaniline can be increased 11 orders of magnitude to about 17 S/cm by complete protonation of the emeraldine base in 1.0 M HCl (pH = -0.2) (17).

Possible Applications

The most attractive application for polyaniline and its derivatives has been electrochemical batteries which use polyaniline as the anodic or cathodic material. Leucoemeraldine base will oxidize to emeraldine base when the battery is charged, and the process is reversed during discharging. The most studied battery type is the lithium/lithium salt/polyaniline battery (1,4-9), since lithium is the lightest metal, and the voltage achieved can be in the range of 3 to 4 V. Polyaniline can also be used as an anode as shown by Kitani (4).

McManus et al. (10) and Kobayashi et al. (11) observed that the electrochromic properties of polyaniline are affected by the pH value. The visual color, as reported by Batich (12), is shown in Table I as a function of pH (degree of protonation) and electrical potential (oxidization state). Mohilner (18) reported that polyaniline changes color as a result of the redox reaction of the film itself. As a result of the electrochromic properties shown in Table I, Kobayashi et al. (13) proposed that a polyaniline film-coated electrode be used as an electrochromic display device by restricting the voltage to values from -0.2 to 0.7 V. Such an electrode which can withstand 10^6 voltage

TABLE I

VISUAL COLORS OF POLYANILINE PREPARED AT VARIOUS pH AND POTENTIAL VALUES

Potential	pH=1	pH=4	pH=7	pH=10	pH=13
-0.2	LY	Y	B	P	RP
0.0	YG	YG	BP	RP	RP
0.4	YG	YG	P	RP	RP
0.7	G	GP	P	RP	RP
1.0	B	B+P	RP	RP	RP
1.4	DB+P	RP	RP	RP	RP

LY : Light Yellow
Y : Yellow
B : Blue
P : Purple
RP : Reddish Purple
YG : Yellowish Green
BP : Bluish Purple
G : Green
GP : Greenish Purple
DB+P: Dark Blue plus some Purple
B+P : Blue plus a little Purple

change cycles, demonstrating that it has the durability for commercialization.

Another successful application was deposition on electrodes to enhance the corrosion resistance (19,20). There are many other applications under study, including ion exchange properties (21), microelectronic devices (22), sensors (23), and electrocatalytic applications (24).

Polyaniline Synthesis

There are two common methods of polyaniline synthesis: (a) classical chemical synthesis and (b) electrochemical synthesis. The aniline monomers in an acid medium are directly oxidized by the appropriate oxidants in the chemical method or by electrical potential during electrochemical synthesis.

The chemical synthesis method was used in this study, since recently reported work leads to the expectation that chemically synthesized polyaniline will provide better processibility than electrochemically produced polyaniline. This follows from the work of Angelopouos et al. (25) who found that polyaniline could be dissolved in 1-methyl-2-pyrrolidinone (NMP). Chemically produced polyaniline "powder" is more readily dissolved in NMP than electrochemically produced "films".

Any shape of free standing emeraldine base can be obtained from solution by evaporating the solvent. Emeraldine base can then be doped to form conducting emeraldine chloride by hydrochloric acid. If desired, the

doped PA can be crystallized by stretching to produce strain-induced orientation to maximize the anisotropy of the electronic and mechanical properties (26,27,28).

There is a variety of chemical oxidants that have been used, including potassium bichromate ($K_2Cr_2O_7$) (29,30), ammonium persulfate ($(NH_4)_2S_2O_8$) (5,31), and sodium persulfate ($Na_2S_2O_8$) (30). The reaction always takes place in an acid medium. Sulfuric acid (29) and hydrochloric acid (5,31) are the most common medium. However, MacDiarmid (31) has suggested using hydrochloric acid, since sulfuric acid will form a non-volatile film on the precipitate particle surface and thereby prevent water escape from the particle during drying. The detailed synthesis procedure, which follows the works of MacDiarmid (31,32), will be described in the next chapter.

Polyaniline Stability

At the beginning of the century, Green and Woodhead (33) mentioned that aniline black (an ill-defined name for polyaniline) could be highly unstable. This soon proved to be incorrect, as Mohilner (18) showed that electrochemically prepared polyaniline was an amorphous powder, stable up to 300°C in air.

The electrochemical synthesis process and the application in rechargeable batteries require an understanding of the film oxidative degradation behavior in aqueous solution. Kobayashi et al. (11) found that degradation was apparent when the potential exceeded 0.7 V

versus a saturated calomel electrode (SCE). The polyaniline reacted with water to form p-benzoquinone. Kobayashi et al. proposed a film degradation mechanism in aqueous solution based on Hand and Nelson's (34) proposed reaction mechanism, as shown in Figure 1. The high anodic potential generated the cation radical ring in the pernigraniline chain. This electrogenerated cation radical ring slowly reacted by hydrolysis in aqueous solution to the quinonediimine cation and quinoneimine radical. The former would undergo further hydrolysis to form quinoneimine, while the latter would undergo further hydrolysis to quinonediimine and p-benzoquinone/hydroquinone mixture.

Oxidation degradation reaction kinetics were also studied by Stilwell and Park (35,36), who observed that the hydrolysis reaction of polyaniline quinonediimine groups to benzoquinone is a function of pH, electrolyte composition and film thickness. The degradation followed the Schiff base hydrolysis mechanism.

The heat-aging of emeraldine hydrochloride has been studied by Hagiwara et al. (17) at 150°C. The electrical conductivity showed the greatest decrease for the case of powder in air, followed by disks in air, and powder in vacuum. These observation show that the oxygen in the air promote the deterioration in conductivity. The original electrical conductivity could not be regained through re-doping the aged emeraldine hydrochloride, even though elemental analysis showed that the chlorine component remained in the aged emeraldine hydrochloride. Further

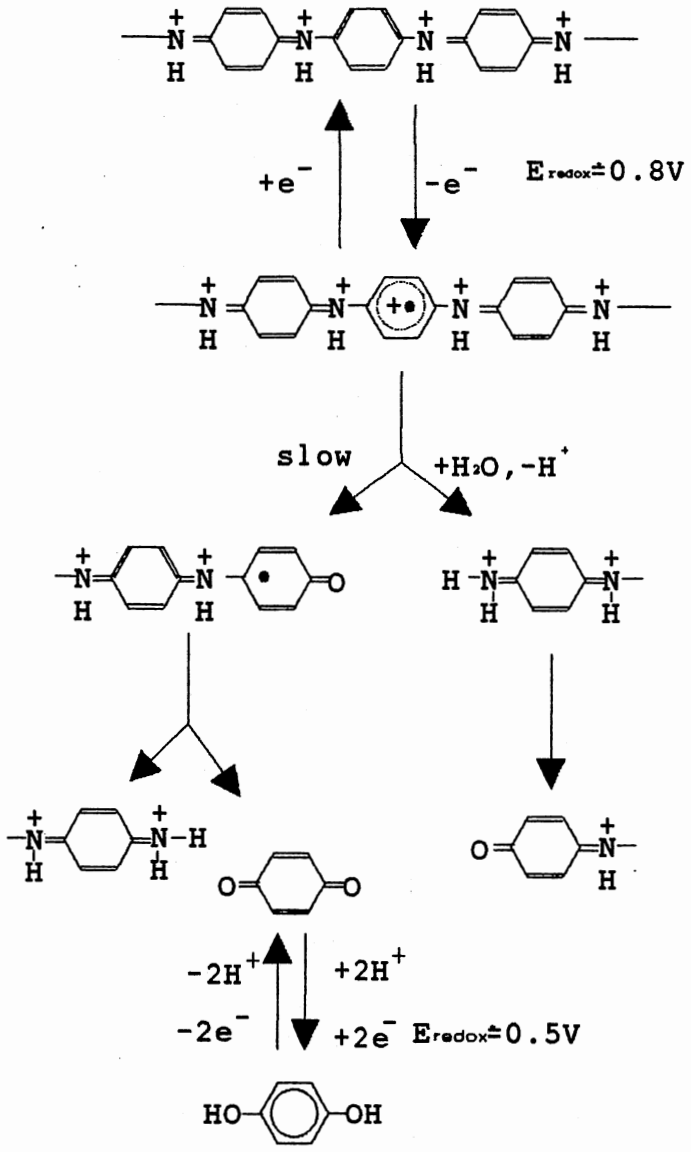

Figure 1. Oxidative Degradation of Polyaniline in an Aqueous Electrolyte

investigation by infrared (IR) and Raman spectroscopy detected the amine structure with a chlorinated aromatic ring. Hagiwara et al. (17) ruled out the idea of a conductivity deterioration mechanism based solely on the loss of the hydrochloric acid from the amino group and proposed a degradation mechanism based on the elimination of hydrochloric acid on the amino group and the simultaneous chlorination of the aromatic ring. As shown in Figure 2, the protonated amine structure was 50% oxidized to high electrical conductivity semiquinone radical-cation structure. The protonated structures were oxidized in the presence of air to the quinoidal structure, which was further oxidized to the deprotonated structure by chlorine substitute.

Film stability was also studied by LaCroix and Diaz (37). The films retained their electrical properties even after remaining in the dry state for 40 days. After remaining at 80°C for 5 days or in 1 M sulfuric acid solution, the films lost their columbic capacity. The films were also subjected to TGA and DSC. Two major weight losses at approximately 60-80°C and approximately 185-195°C were observed, the first was attributed to moisture loss, and the latter to decomposition. Mass spectroscopy confirmed that water is the only volatile component released from the sample during heating below 100°C. When the TGA curve was compared with DSC curve, there was an exothermic peak at 80-110°C before weight loss of water. This was not explained by the authors.

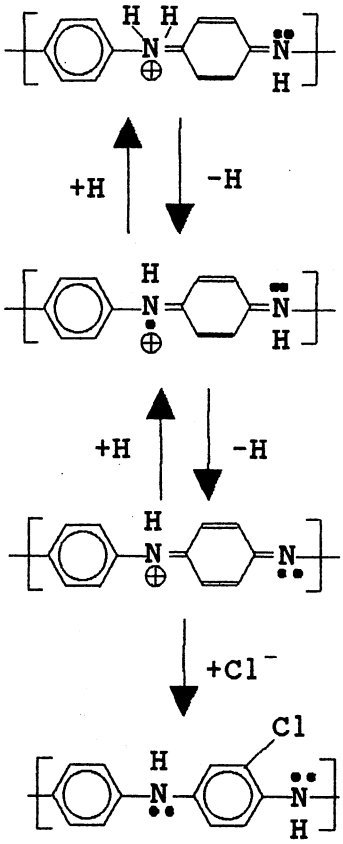

Figure 2. Chlorination of Aromatic Ring in Polyaniline

The same results were observed by Wei and Hsueh (38) for different aging conditions. They observed that there was no water coming out of the emeraldine base below 100°C, and explained that the water molecules in the emeraldine hydrochloride could be weakly bonded to the sites which were otherwise occupied by Cl^-. Gel-permeation chromatography (GPC) showed a molecular weight shift to the higher end, indicating crosslinking after aging at 200°C for 6 hours. If this proposition is true, the LaCroix and Diaz observation of the DSC exothermic peak before the water release could be attributed to crosslinking.

A polymer molecule chain can be broken down into fragments by the following mechanisms:

(a) random degradation, where bonds in the chain are broken at random;

(b) unzipping, where chain scission is the reverse of addition polymerization and monomer units are released successively from a chain end or at a weak link near the chain end;

(c) weak-link degradation, where chain scission occurs at weak links distributed at random along the backbone, which are more easily ruptured than normal bonds.

The polymer chain scission was investigated by Traore et al. (39) by putting emeraldine hydrochloride through TGA under high vacuum conditions (10^{-5} Torr) in conjunction with thermal volatilization analysis (TVA), to study the back bone decomposition behavior at higher temperatures. The hydrogen chloride gas achieved maximum evolution rate from

emeraldine chloride at about 230°C at a heating rate of 10°C/min. The scission reaction between reduced mers began at 520°C to 740°C, and produced ammonia, aniline, p-phenylenediamine, N-phenylaniline, and N-phenyl-1,4-benzenediamine. The reaction scheme is shown in Figure 3. The remaining reduced repeating units fused to carbazole at higher temperatures and released hydrogen gas. The ladder structure of carbazole group can withstand higher temperatures without decomposition. The oxidized repeating units under went scission and rearranged to a pyridine-based heterocycle below 650°C. The oxidized repeating units decomposed to ammonia, methane, and acetylene above 730°C.

Yue et al. (40) compared the thermostability of emeraldine hydrochloride and sulfonated emeraldine to their insulating forms. The sulfonated emeraldine still showed two major weight loss regions on the TGA curve. Yue et al. suggested that the mechanism resulting in two major weight losses was similar to the hydrochloride emeraldine degradation mechanism, but with sulfonic acid emission instead of hydrochloric acid emission. The insulating form showed more stability than the conducting form as evidenced by its TGA curve. The increased stability was attributed to the covalently bonded sulfonic groups on the emeraldine chain.

Kinetic Parameters

The kinetic parameters of polymer degradation, namely the activation energy, ΔE, and the pre-exponential factor A,

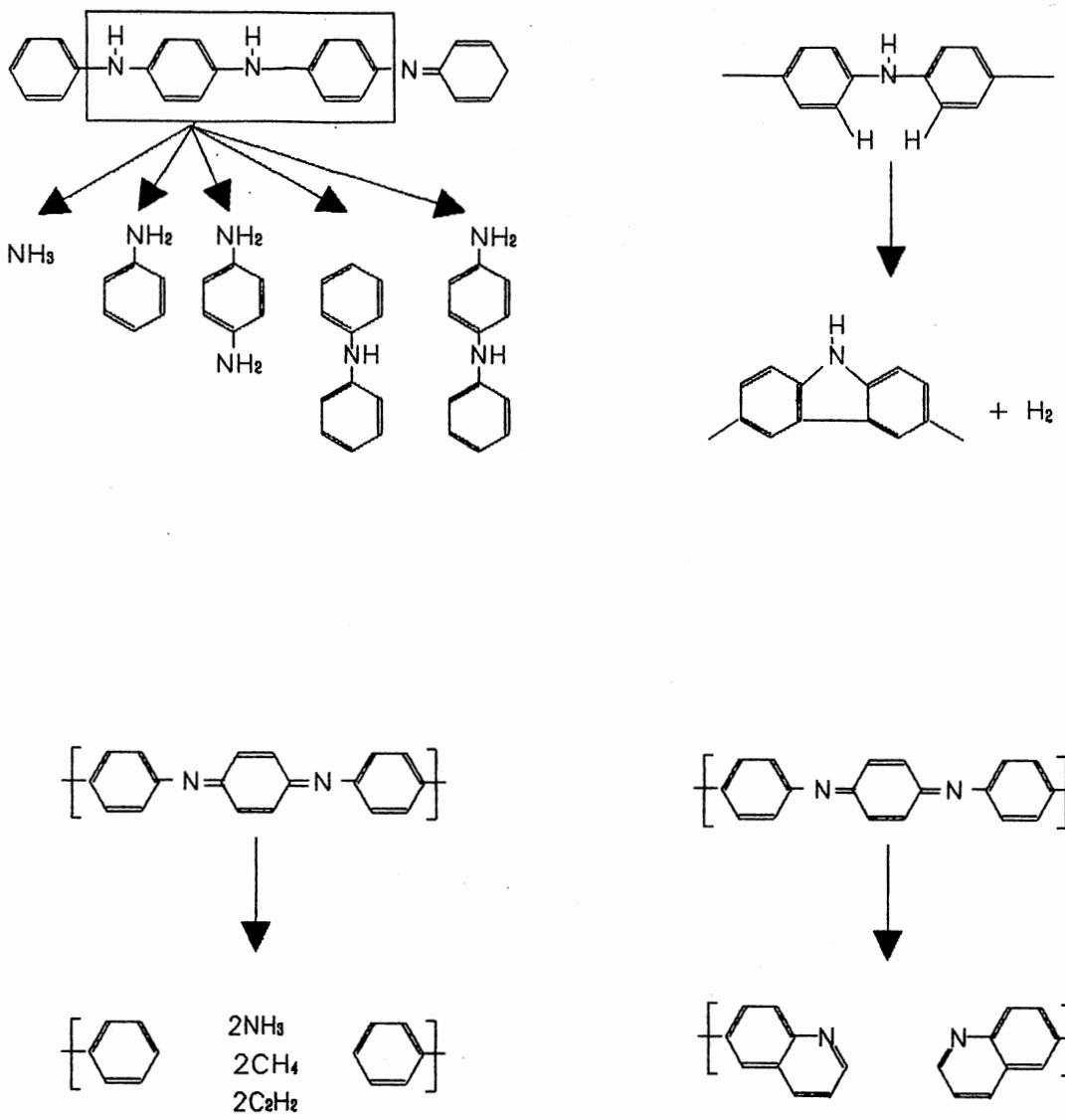

Figure 3. Backbone Decomposition Reaction of Polyaniline

have been commonly evaluated by TGA. TGA gives a record of residual weight versus temperature for a sample heated at a constant rate under a particular set of experiment conditions. There is a variety of methods to evaluate kinetic parameters from these curves. After comparison of different methods, Flynn and Wall (41) concluded that a single TGA curve is applicable to systems in which reaction orders are known and the decomposition products volatilized by the same kinetic process. Flynn and Wall suggested a method involving different heating rates. In this work the kinetic parameters were determined by the method of Ozawa (42), which uses four different heating rate curves.

The rate of decomposition has the following form:

$$-\frac{dW}{dt} = k\, W^n \qquad (1)$$

where W = fractional residual weight of the sample

t = time

n = the order of the reaction

k = rate constant.

In the TGA experiment, the temperature dependence is assumed to reside in the rate constant through an Arrhenius's type relation. The kinetic equation then becomes

$$-\frac{dW}{dt} = A \exp\left(\frac{-\Delta E}{RT}\right) W^n \qquad (2)$$

where R = ideal gas constant

T = absolute temperature

A = pre-exponential factor

ΔE = the apparent activation energy.

W^n can be expressed as $g(W)$.

The kinetic equation then becomes:

$$-\frac{dW}{dt} = A \exp\left(\frac{-\Delta E}{RT}\right) g(W) . \qquad (3)$$

By rearrangement and integration

$$-\int_{W_o}^{W} \frac{dW}{g(W)} = A \int_{t_o}^{t} \exp\left(\frac{-\Delta E}{RT}\right) dt \qquad (4)$$

Since $T = a\ t + T_0$ at a constant heating rate, a, it followed that $dT = a\ dt$. The kinetic equation can be changed to the following form by change the variable time t to temperature T.

$$-\int_{W_o}^{W} \frac{dW}{g(W)} = \frac{A}{a} \int_{T_o}^{T} \exp\left(\frac{-\Delta E}{RT}\right) dT \qquad (5)$$

where T_0 is the value of T at $t=t_0$. Generally the reaction rate is very low at low temperatures and the lower limit at the right hand side integration can be approximated as zero:

$$-\int_{W_o}^{W} \frac{dW}{g(W)} = \frac{A}{a} \int_{0}^{T} \exp\left(\frac{-\Delta E}{RT}\right) dT . \qquad (6)$$

Integration of the right hand side of Equation 6 results in

an infinite series of the form:

$$\int_0^T \exp\left(\frac{-\Delta E}{RT}\right) dT = \frac{\Delta E}{R}\left[\frac{\exp\left(\frac{-\Delta E}{RT}\right)}{\frac{\Delta E}{RT}} + \left(\ln\frac{\Delta E}{RT} - \frac{\Delta E}{RT} + \cdots\right)\right]. \quad (7)$$

Doyle (43) has represent the series by the following expression:

$$\int_0^T \exp\left(\frac{-\Delta E}{RT}\right) dT = \frac{\Delta E}{R}\, p\left(\frac{\Delta E}{RT}\right) \quad (8)$$

and shown that p is well approximated by

$$\log_{10} p\left(\frac{\Delta E}{RT}\right) \approx -2.315 - 0.4567\left(\frac{\Delta E}{RT}\right) \quad (9)$$

when $\Delta E/RT > 20$. The kinetic equation (Equation 5) then becomes

$$-\int_{W_o}^{W} \frac{dW}{g(W)} = \frac{A\ \Delta E}{a\ R}\, p\left(\frac{\Delta E}{RT}\right) . \quad (10)$$

For a given value of W, the left hand side of the kinetic equation is a constant, independent of the heating rate and the reaction order. Therefore, for a given weight fraction, the right hand side of Equation 10 evaluated at $T=T_1$ for a heating rate of a_1, must be equal to the right hand side of Equation 10 evaluated at $T=T_2$ for the heating rate a_2. That is:

$$\frac{A\Delta E}{a_1 R}\, p\left(\frac{\Delta E}{RT_1}\right) = \frac{A\Delta E}{a_2 R}\, p\left(\frac{\Delta E}{RT_2}\right) = \bullet\bullet\bullet \qquad (11)$$

provided that W is constant. Using Doyle's approximation and taking the logarithm, the following linear equation can be obtained:

$$-\log_{10} a_1 - 0.4567\frac{\Delta E}{RT_1} = -\log_{10} a_2 - 0.4567\frac{\Delta E}{RT_2} = \bullet\bullet\bullet \qquad (12)$$

The activation energy can be obtained from the slope of the $\log_{10} a$ versus the reciprocal absolute temperature plots at a given value of W.

The next step in the analysis is to determine the value of A and the reaction order. Once ΔE has been determined, the right hand side of Equation 10 can be evaluated except for A. By plotting W as function of $\log\{(\Delta E/aR)p(\Delta E/RT)\}$, a curve is obtained which should superimpose, when linearly shifted, onto one of the curves given in Table II, thereby determining the reaction order. The length of the lateral shift is equal to $\log_{10} A$.

TABLE II

SOME TYPICAL FORMS OF $g(W)$ AND $-\int_{W_o}^{W} \frac{dW}{g(W)}$

Type of reaction	$g(W)$	$-\int_{W_o}^{W} \frac{dW}{g(W)}$
0th order	1	$W_o - W$
1st order	W	$\ln(W_o/W)$
2nd order	W^2	$1/W - 1/W_o$
3rd order	W^3	$2/W^2 - 2/W_o^2$
4th order	W^4	$3/W^3 - 3/W_o^3$

CHAPTER III

EQUIPMENT, MATERIALS, AND PROCEDURES

This chapter describes the methods and equipment used to produce the polyaniline samples, measure the degradation kinetics, and identify the reaction products.

Thermogravimetric Analysis (TGA)

The Cahn TGA system 113 used in this study is shown schematically in Figure 4. The sample was placed in the stirrups and subjected to a constant heating rate while the temperature and weight were measured and recorded. The temperature was controlled by a MICRICON 823 temperature controller and ramp generator. The sample weight was measured by the weighing unit which was controlled by a CAHN 2000 control unit. For the convenience of further analysis, the temperature and the weight signals were digitized by a DAS-8 analog to digital (A/D) board and stored in a computer for later reduction. The functions of the EXP-16 were: conjunction compensation for the thermocouple and amplification of the 100 mV weight signal from the Cahn 2000 control unit to a 5 V signal for the DAS-8.

TGA Procedure

(1) The parameters of the temperature control unit

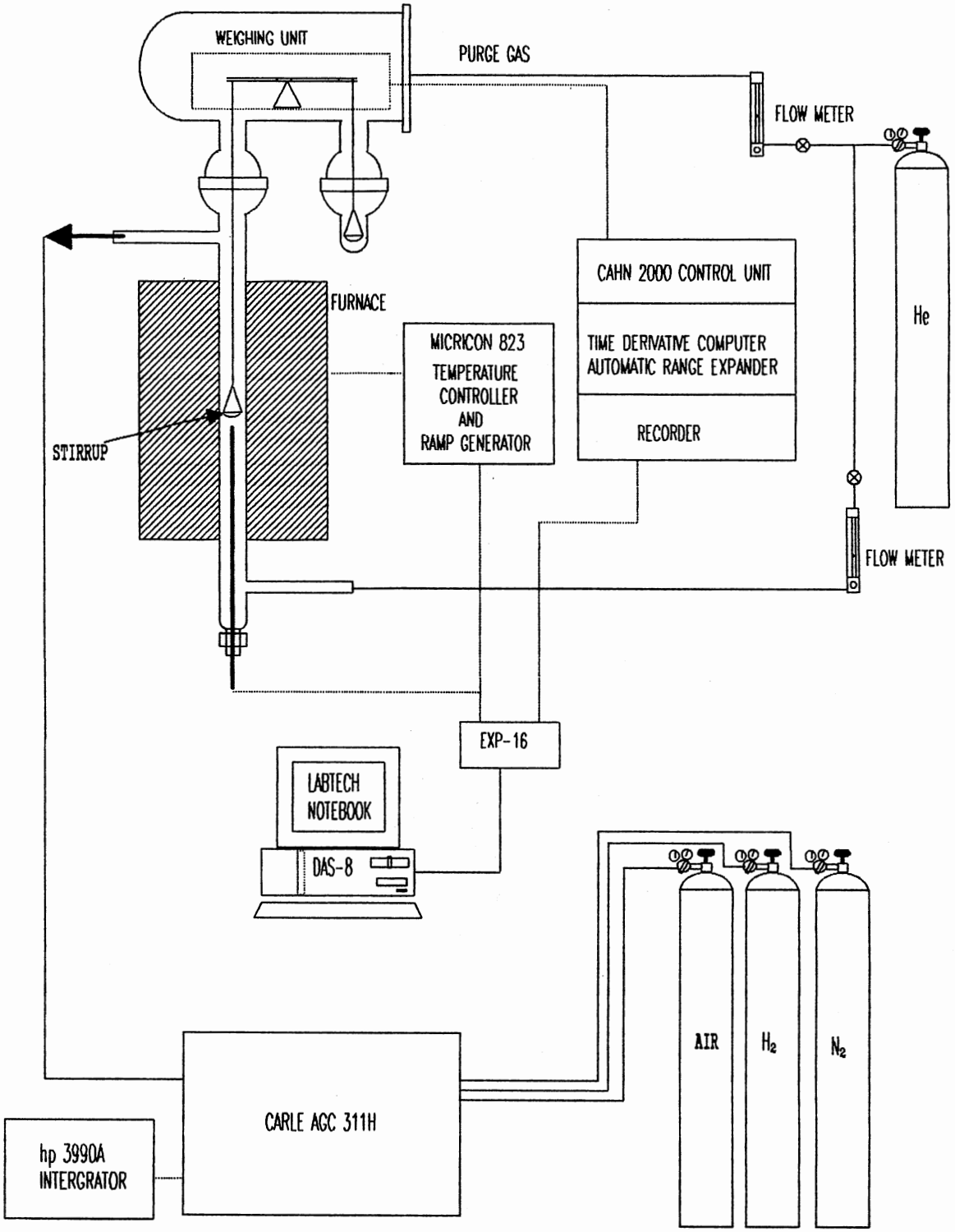

Figure 4. Experimental Setup

(MICRICON 823) were set; an example of the parameters for a heating rate of 10°C/min from 25 to 925°C is given in Table III.

(2) The parameters which corresponded to the heating rate above in the data acquisition system (LABTECH NOTEBOOK) were set; an example of parameters at heating rate of 10°C/min is given in Table IV.

(3) The weight control unit was zeroed under vacuum to avoid the error caused by air buoyancy.

(4) Approximately 8 mg of sample was weighed into the stirrup.

(5) The stirrup with the sample was placed on the hangdown wire, and the hangdown tube was closed. Static electricity was removed by an ionizing unit which produced alpha particles.

(6) Due to the restriction of the DAS-8/EXP-16, the recorder range was selected to give a response in the range of 100 mV.

(7) The vacuum pump was switched on.

(8) The MICRICON 823 temperature control unit was activated.

(9) The NOTEBOOK data acquisition unit was started.

(10) Upon reaching the final temperature, the whole TGA system was switched off and the data was saved on a floppy disk for later analysis.

(11) Steps 1 to 10 were repeated for three additional heating rates.

TABLE III

EXAMPLE OF PARAMETER SETTINGS FOR MICRICON 823

Parameter			Value
Controller			
	Gain		64
	Reset		4
	Rate		1
Programmer		PR 1	STM	NEXT
	SEGM 1	25	0.1	2
	SEGM 2	25	3	3
	SEGM 3	925	90*	4
	SEGM 4	925	5	4

SEGM : segment

PR : profile

STM : segment time; min

* This value changes according to the heating rate.

TABLE IV

EXAMPLE PARAMETER SETTINGS FOR NOTEBOOK

Parameter	value		
Channel			
Channel number	1	2	3
Channel name	Temperature	Weight	Time
Channel type	Thermocouple	Analog input	time
Interface channel number	16	17	18
Sampling rate, HZ	.333*	.333*	.333*
Stage duration, sec	6000*	6000*	6000*
Window			
Window number	1	2	
Left limit	0.1	0.1	
Lower limit	0.55	0.15	
Right limit	0.99	0.99	
Upper limit	0.99	0.55	
X tic start value	0.0	0.0	
X tic end value	6000*	6000*	
Y tic start value	0.0	-20.0	
Y tic end value	6000*	6000*	
File			
File name	EB10_2.PRN*		

* These values changed according to the heating rate.

Gas Chromatograph (Carle AGC 311H)

Due to the lack of documentation for the Carle gas chromatograph, it is necessary to discuss this instrument in detail. The Carle GC can be divided into two systems, the flame ionization detector (FID) and thermal conductivity detector (TCD) as seen in Figure 5. Since the FID was insensitive to the components of the degradation products, the FID system was not used in the analysis procedure. The sampling valve 2 (V2) was a combination of back flushing and sampling valve which changed the flow directions in column 3 by switching the valve. The analysis columns were #3 and #4, and were packed with 10 feet mesh 60/80 HayeSep C and 9 feet mesh 45/60 molecular sieve 5A, respectively. The HayeSep C column provided the separation of ammonia, acetylene, carbon dioxide, and heavier components from the others. The molecular sieve provided the separation of light components, such as methane, carbon monoxide, and hydrogen. As shown in Figure 5, there are 2 valves in the TCD system. When valve 3 was turned clockwise the components in molecular sieve were trapped, since no helium can flow through, and the effluent gas from column 3 was bypassed from column 4 to the TCD. This feature had the advantage of allowing separation of two totally different sets of component types in one run. This GC was also equipped with a hydrogen transfer system (HTS). Due to the high thermal conductivity of hydrogen, hydrogen always gives negative deflection in the chromatogram and low sensitivity

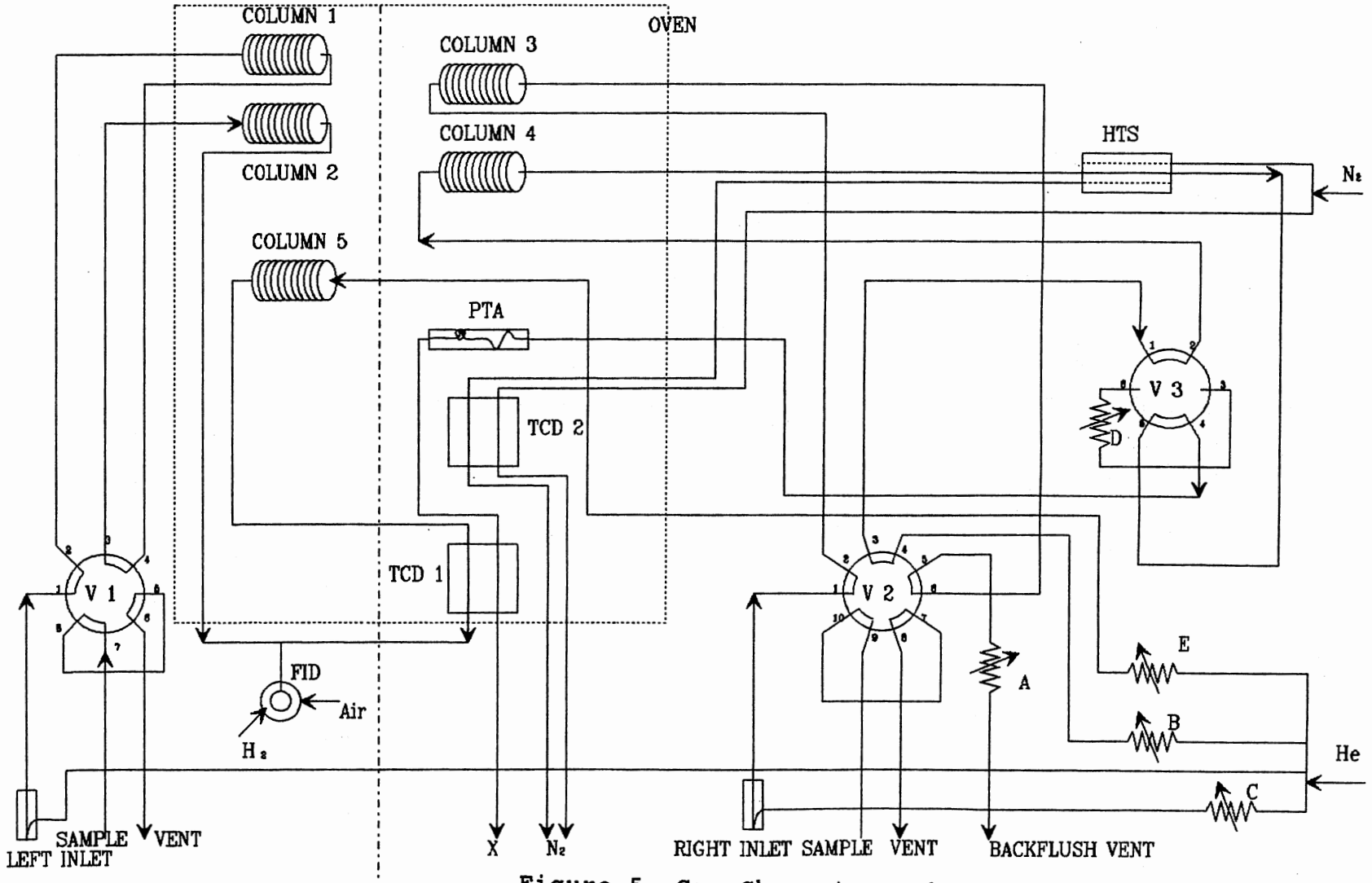

Figure 5. Gas Chromatograph

in the helium carrier gas. The HTS was utilized to give a positive deflection, and improve the sensitivity and linearity to concentration.

The method used for analysis was to elute the hydrogen first with valve 2 in the clockwise position and valve 3 in counter clockwise position. The valves shown in Figure 5 are in the counter clockwise positions. The carbon monoxide and methane in the molecular sieve were trapped in the column by switching valve 3 to the bypass position (clockwise). At that time ammonia, acetylene, and carbon dioxide were analyzed. After the ammonia was eluted from the HayeSep column, the heavier components in the HayeSep column were backflushed by bringing valve 2 to the counter clockwise position. The components trapped in the molecular sieve column were then analyzed by switching valve 3 to the counter clockwise position.

The retention times for different components are very important in determining the valve switching time and in identifying the components from the chromatogram. The retention times are shown in Table V. Care should be taken to prevent acetylene, carbon dioxide, and ammonia from entering molecular sieve column, since they will be permanently adsorbed by the molecular sieve at the operation temperature. The analysis procedure is as follows:

(1) A fixed amount of sample was injected into the GC by a Pressure-Lock gas syringe, and the integrator was simultaneously started.

(2) Valve 3 was turned to the clockwise position after

TABLE V

RETENTION TIMES FOR THE COMPONENTS ANALYZED

Component	Retention time, min
Hydrogen	2.52
Oxygen	3.93
Nitrogen	5.02
Methane	6.85
Carbon monoxide	10.23
Carbon dioxide	3.01
Acetylene	4.20
Ammonia	4.40

(a) The retention time of acetylene, carbon dioxide, and ammonia were measured by only passing through the HayeSep column.

(b) Operation conditions:

Oven temperature = 100°C

HTS temperature = 600°C

Helium flow rate = 30 ml/min.

(c) The interpretation of gas chromatogram can refer to Appendix E.

2.75 min.

(3) Valve 2 and valve 3 were turned to the counter clockwise position after the ammonia was eluted (5.0 min).

(4) The integrator was stopped after carbon monoxide was eluted.

(5) At this point of time, the GC was ready for another injection.

Material Preparation Procedure

Emeraldine base was prepared by the method of chemical oxidization as described below (31,32).

(1) 1 liter of 1 M HCl solution was prepared.

(2) Aniline was distilled under vacuum to remove any impurities caused by photo-degradation.

(3) 20 ml (0.219 mole) of purified aniline monomer ($C_6H_5NH_2$) was dissolved in 300 ml of 1 M HCl and cooled to 1°C in an ice bath to form a 0.684 M solution of aniline.

(4) 11.5 g (0.05 mole) of the oxidant, ammonium persulfate ($(NH_4)_2S_2O_8$), was dissolved in 200 ml of 1 M HCl and cooled to 1°C. to form a 0.25 M ammonium persulfate solution.

(5) The aniline solution from step 3 was placed in a 750 ml Erlenmeyer flask with a magnetic stirring bar, and the container was placed in an ice bath on a magnetic stirring plate.

(6) The ammonium persulfate solution from step 4 was slowly

added to the aniline solution with constant stirring over 1 min. period. A blue-green precipitate appeared on the flask wall after 3 to 5 min of stirring.

(7) The solution was stirred continuously in the ice bath while the temperature was controlled below 5°C for approximately 1.5 hours.

(8) The precipitate was collected on a Buchner funnel by aspiration.

(9) The precipitate cake was washed portion-wise (60 ml/portion) with 500 ml of 1 M hydrochloric acid until the initially pale violet filtrate turned colorless. Care was taken to insure that the liquid level remained above the top of the precipitate to prevent the cracking of precipitate cake.

(10) After washing the precipitate, the vacuum remained on for approximately 10 min.

Conversion to Fully Protonated Emeraldine Hydrochloride

Since the as-made emeraldine base contained oxidant, it needed to be purify and brought to the fully protonated form by the following procedure.

(11) The precipitate cake was suspended in 500 ml of 1 M HCl with constant stirring for approximately 15 hours.

(12) Steps 8 to 10 were repeated.

(13) The filter paper was transferred to a vacuum desiccator and held under vacuum for 4 hours.

(14) The precipitate was manually pulverized by mortar and pestle and dried under dynamic vacuum for approximately 48 hours.

The Final Stage in the Preparation of Emeraldine Base

(15) The precipitate was added to 500 ml of 0.1 M ammonium hydroxide (NH_4OH) solution and stirred for approximately 15 hours while the pH was maintained at 8 or greater.

(16) The precipitate was collected in a Buchner funnel and washed with 500 ml of 0.1 M ammonium hydroxide in 60 ml portions.

(17) The powder was resuspended in an additional 500 ml of 0.1 M ammonium hydroxide and stirred for approximately 1 hour.

(18) The precipitate was separated in a Buchner funnel and washed with 500 ml of 0.1 M ammonium hydroxide in 60 ml portions.

(19) The precipitate was dried in the Buchner funnel under vacuum for 10 min.

(20) The precipitate was then transferred to a dynamic vacuum desiccator for approximately 4 hours.

(21) The precipitate was manually pulverized and dried under dynamic vacuum for 72 hours. This emeraldine base precipitate was the material for the degradation study.

The Procedure for Preparing Sulfonate Emeraldine (40)

(1) Emeraldine base was dissolved in 40 ml of fuming sulfuric acid with constant stirring for approximately 2 hours. Upon sulfonation the color slowly turned from dark purple to dark blue.

(2) The solution was slowly added to 200 ml of methanol over a period of approximately 20 min. while kept it in

an ice bath whose temperature remained between 10-20°C.

(3) 100 ml of acetone was added to the solution of step 2.

(4) The precipitate was separated in a Buchner funnel and it was washed with ten 50 ml portions of methanol until the pH equaled 7.

(5) The precipitate cake remained under suction for approximately 10 min.

(6) The cake was transferred to a desiccator and dried under dynamic vacuum for 24 hours.

The material was then ready for thermodegradation analysis.

CHAPTER IV

RESULTS AND DISCUSSION

The experimental results presented in this chapter, consists of TGA and GC experiments. Polyethylene was tested first for the purpose of verifying the Ozawa integration method. The polyethylene thermodegradation was carried out from temperatures of 25 to 625°C, under vacuum at four different heating rates. The resulting TGA curves are shown in Figure 6. The four polyethylene thermogravimetries were plotted against the reciprocal of the absolute temperature, as shown in Figure 7. For a given residue weight fraction, there are different reciprocal temperatures at different heating rates. The logarithms of the heating rates were plotted against the reciprocal of the absolute temperature with weight fraction as a parameter in Figure 8. The activation energy, ΔE, was obtained from the slopes which were determined by linear regression, as shown in Table VI. By using the determined activation energy (61.2 kcal/mole), the weight changes were plotted against $\log[(\Delta E/aR)p(\Delta E/RT)]$ and compared with the curves for different reaction orders as shown in Figure 9. The decomposition mechanism follows the 1st order reaction, and the lateral shift length (log A) is also listed in Table VI. The average pre-exponential factor was 4.5×10^{17} min^{-1}. The measured kinetic parameters

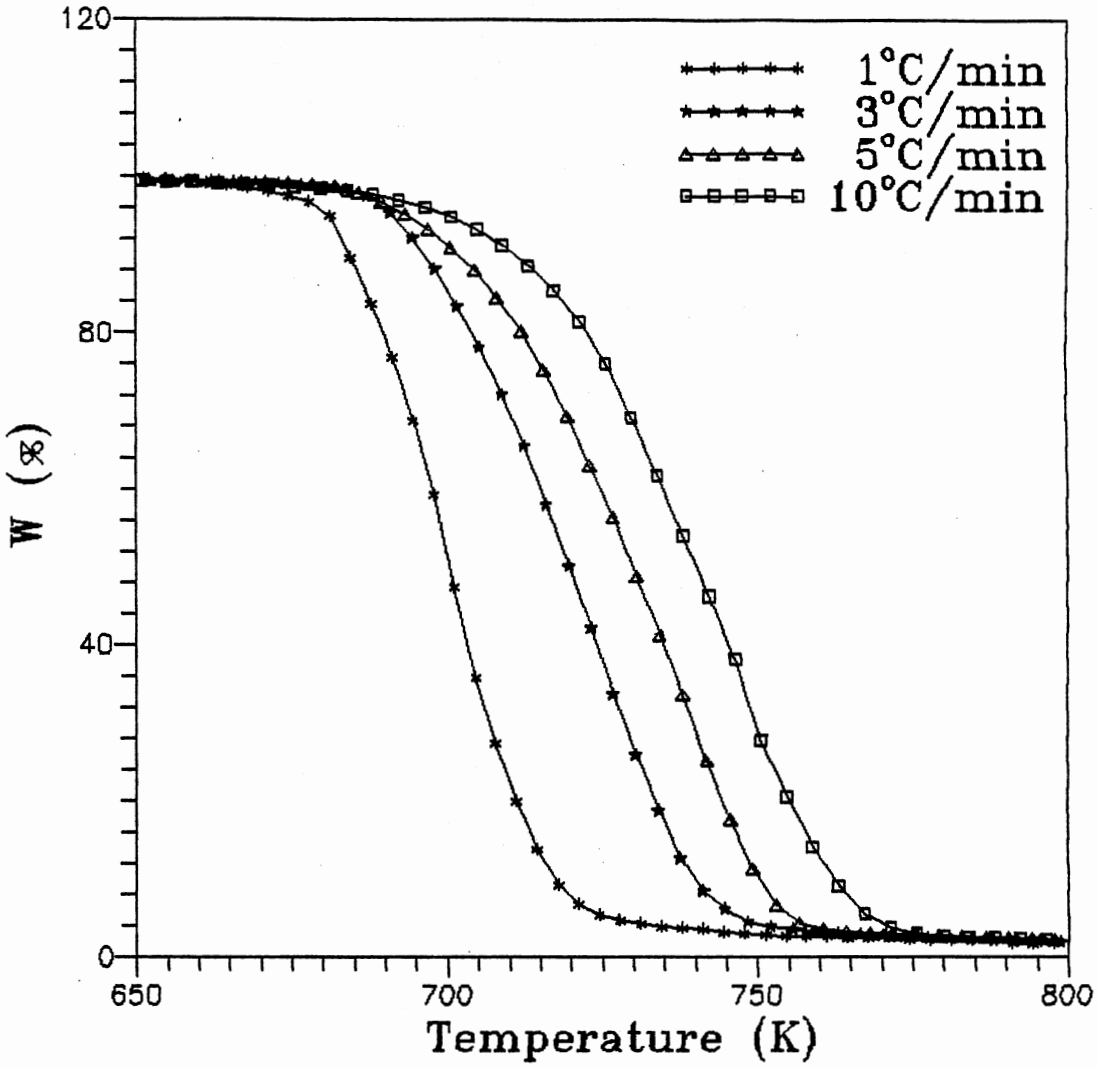

Figure 6. TGA Curves of Polyethylene at Various Heating Rates

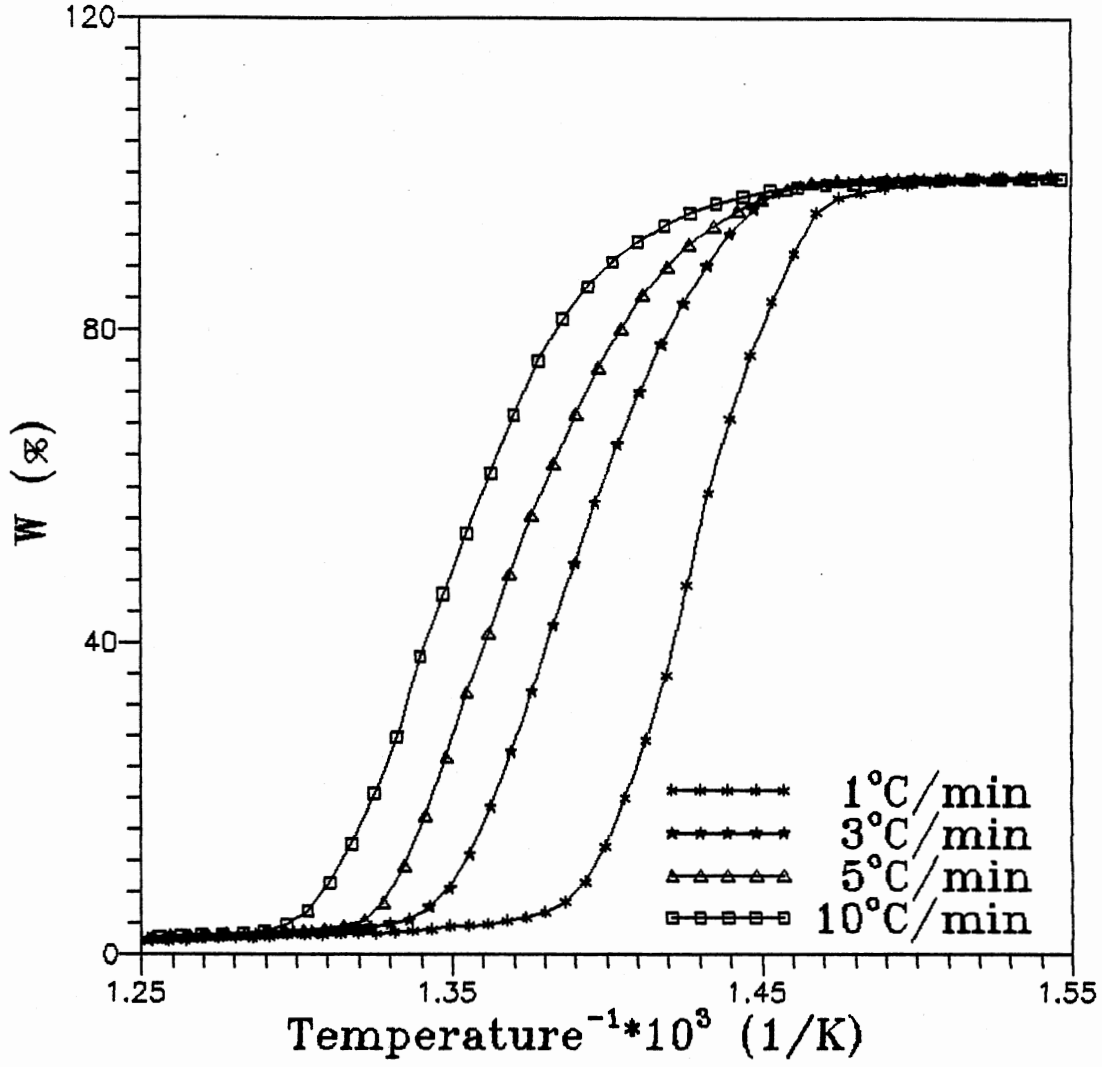

Figure 7. Thermogravimetric Curves of Polyethylene as a Function of the Reciprocal Absolute Temperature

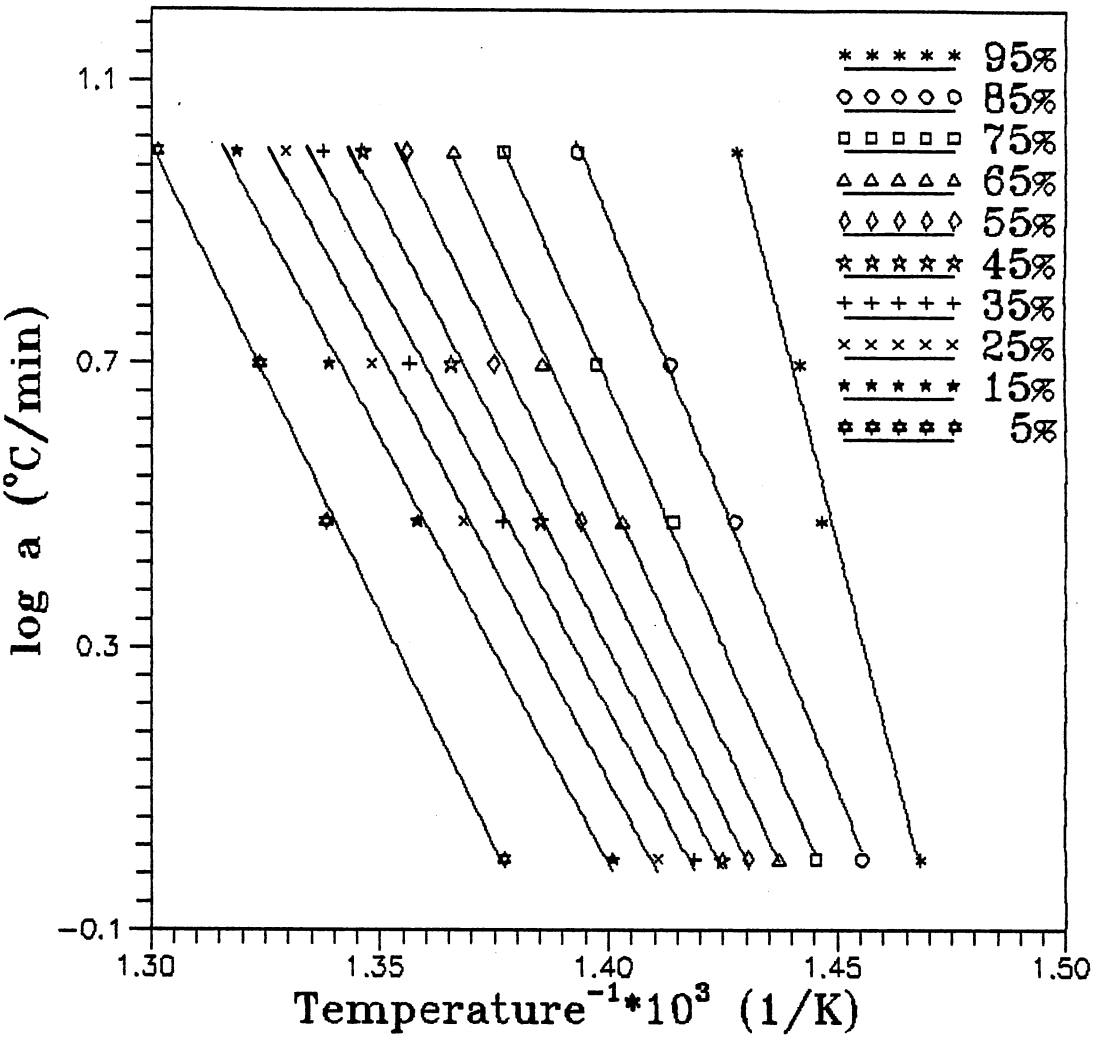

Figure 8. Plots of Logarithmic Heating Rate Against the Reciprocal Absolute Temperature for Different Conversions of the Decomposition of Polyethylene

TABLE VI

KINETIC PARAMETERS OF THE DECOMPOSITION OF POLYETHYLENE

W	slope	ΔE	log A
0.95	-25.232	109779.7	17.4281
0.90	-18.456	80296.2	17.5439
0.85	-16.119	70129.3	17.5948
0.80	-15.119	65777.2	17.6255
0.75	-14.584	63449.6	17.6463
0.70	-14.239	61948.5	17.6625
0.65	-13.911	60521.9	17.6743
0.60	-13.579	59078.8	17.6819
0.55	-13.181	57349.3	17.6877
0.50	-12.829	55817.9	17.6924
0.45	-12.511	54430.4	17.6952
0.40	-12.230	53209.1	17.6975
0.35	-12.051	52429.9	17.7017
0.30	-12.068	52506.9	17.7048
0.25	-12.051	52429.5	17.7058
0.20	-11.988	52157.1	17.7046
0.15	-11.981	52126.7	17.7017
0.10	-12.007	52240.7	17.6946
0.05	-13.214	57490.3	17.6327
mean		61234.4	17.6566
		A	4.5×10^{17}

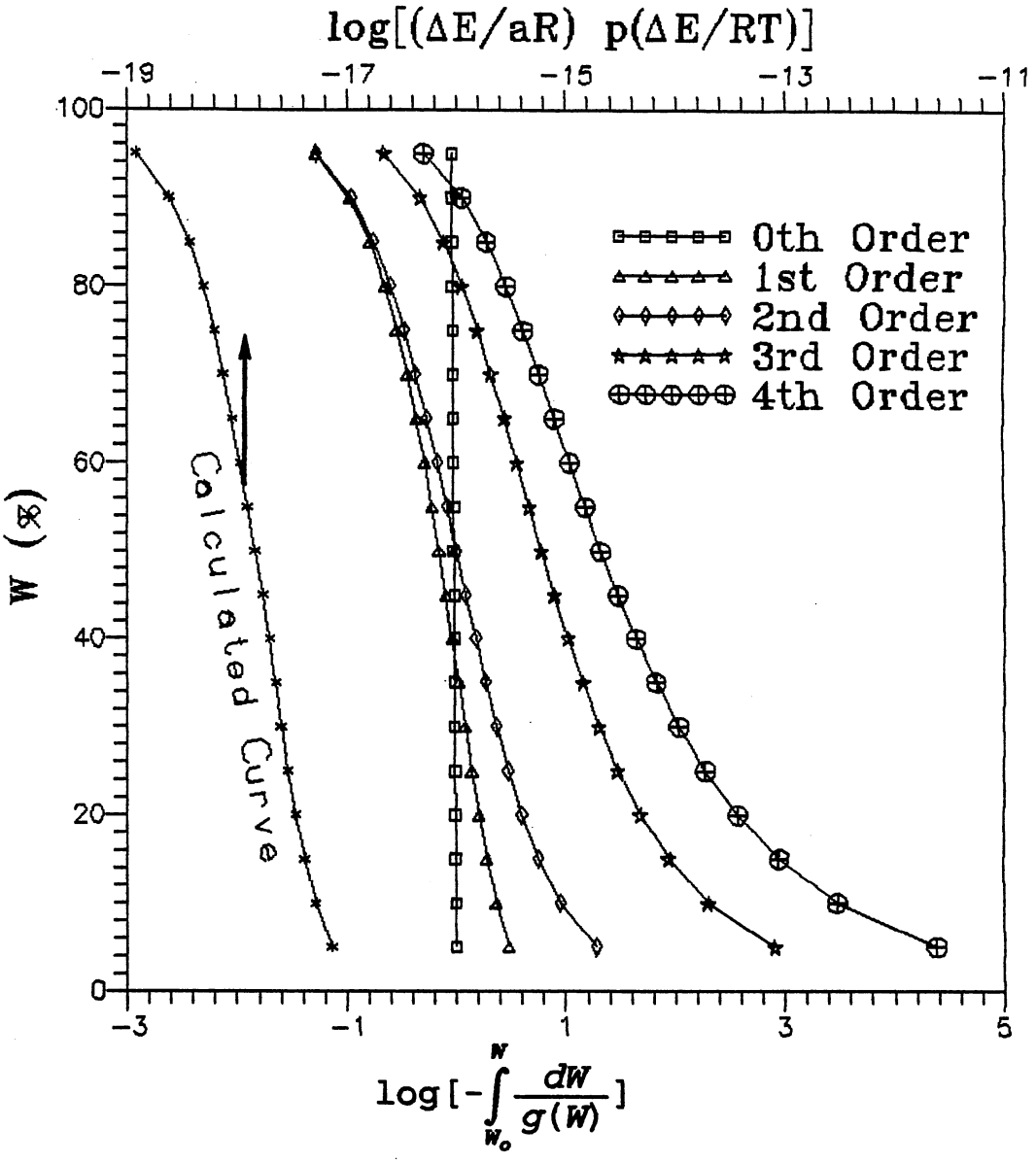

Figure 9. Comparison of the Calculated Curve with Different Reaction Orders for Polyethylene

were used to calculate the residue weight versus temperature by theoretical equation (Equation 10) and compared with the experimental data, as shown in Figure 10. The calculated activation energy was consistent with the Madorsky (44), and Oakes and Richards (45) papers, both of which stated that the order of decomposition reaction was 1st order, and the activation energy was 68±5 kcal/mole and 60-70 kcal/mole, respectively. In the paper by Andersons (46), the first 3 percent of weight loss was 0th order and 48 kcal/mole given as the activation energy; the weight loss from 3-15% was 1st order and 61 kcal/mole reported as the activation energy, after 35% weight loss the reaction followed 1st order kinetics and ΔE = 67 kcal/mole. The results of the present experiment were consistent with the data of these papers.

The same analysis procedure was applied to emeraldine base. The results of emeraldine base TGA curves from 25 to 925°C under vacuum at four different heating rates are shown in Figure 11. The detail used calculation graphs and table can refer to Figures 12 and 13, and Table VII. The reaction order, activation energy ΔE, and pre-exponential factor were obtained as 2nd order, 30.4 kcal/mole, 2.73×10^{6} min^{-1}, respectively. These kinetic parameters were used to calculate the residue weight versus temperature from the theoretical equation and compared with the experiment data, as shown in Figure 14. The calculated data fit the experimental data with an offset of approximately 7°C. One possible reason for the offset could be the assumption in Doyle's approximation that $\Delta E/RT$ be greater than 20. The

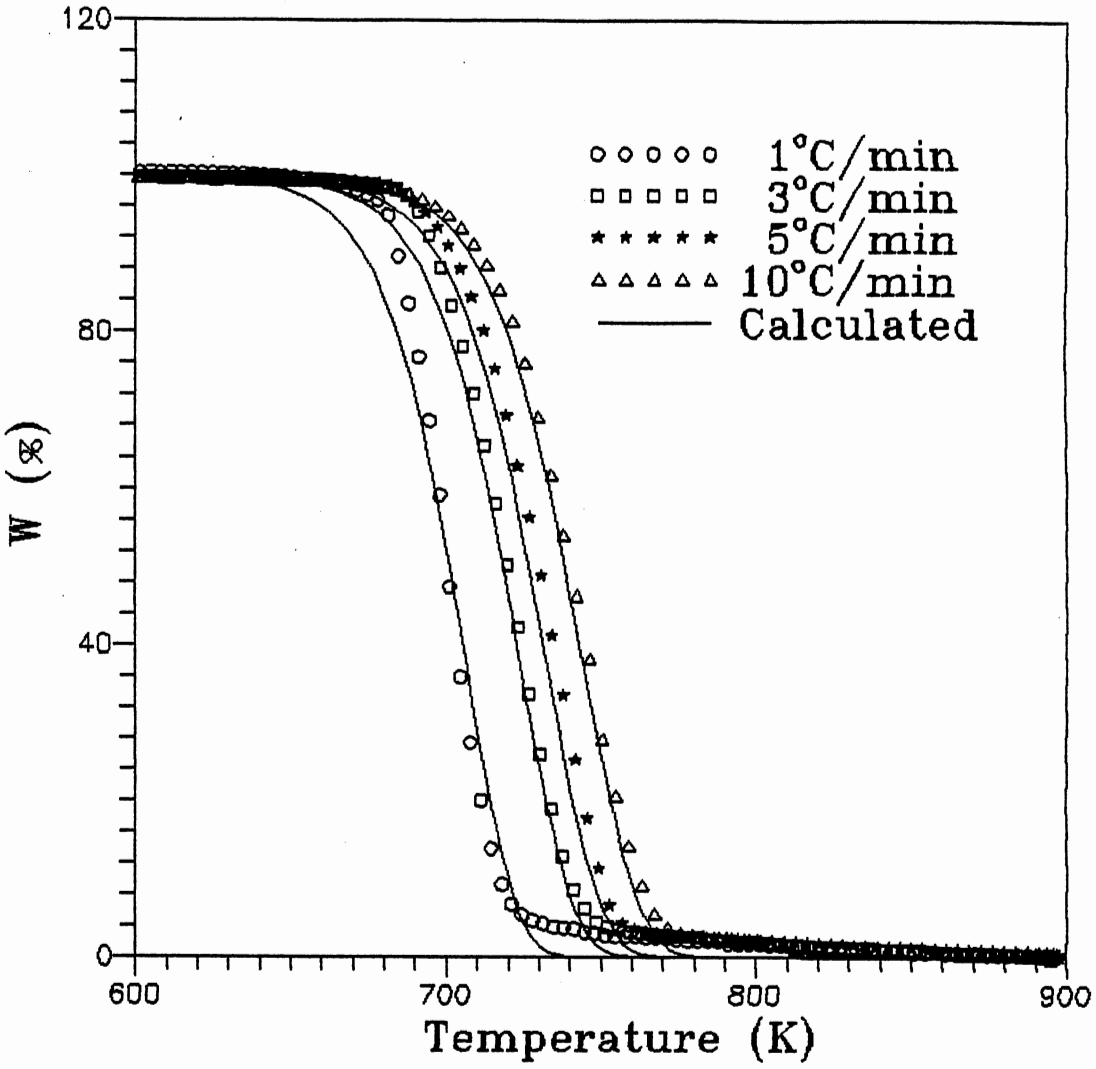

Figure 10. Comparison of Experimental and Calculated TGA Curves of Polyethylene

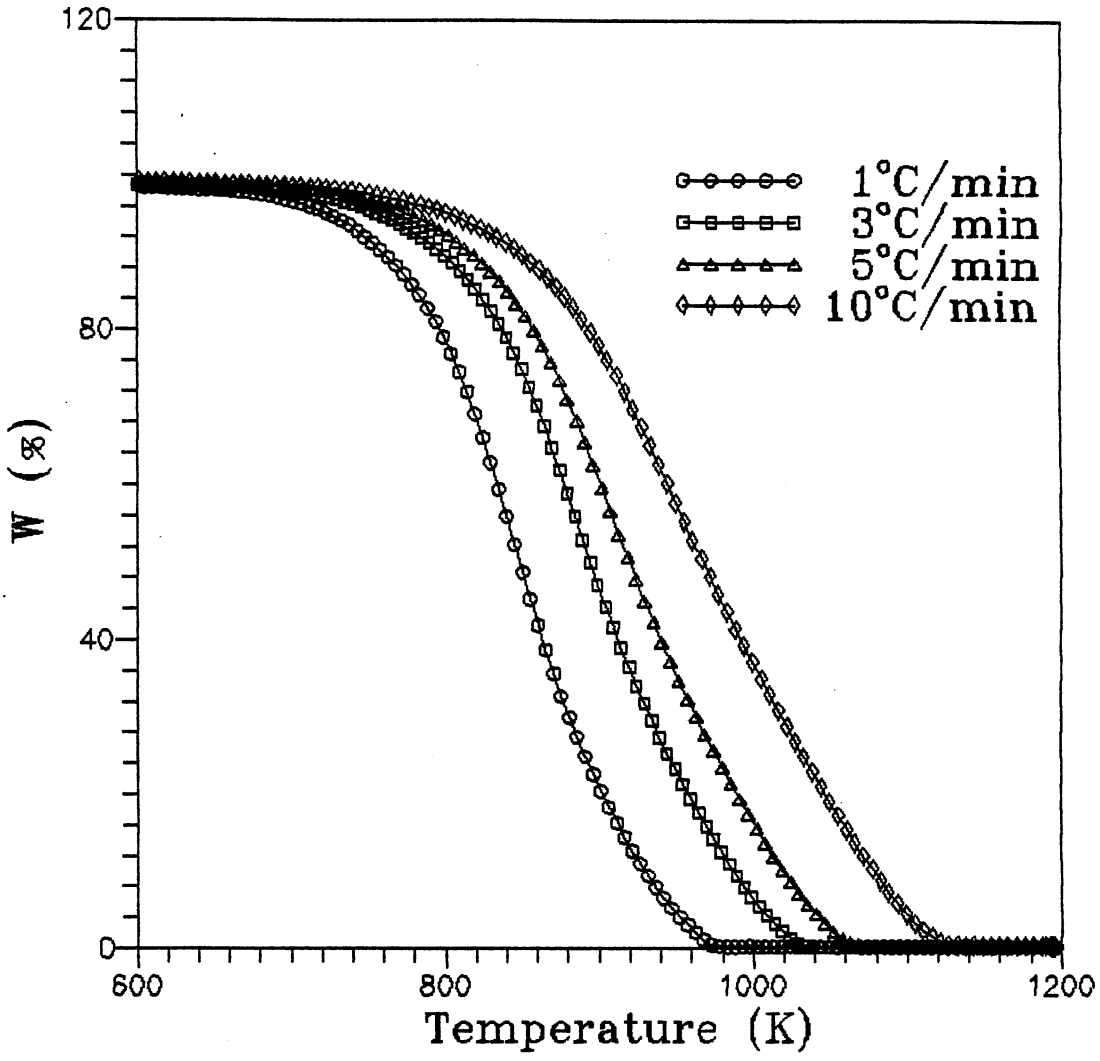

Figure 11. TGA Curves of Emeraldine Base at Various Heating Rates

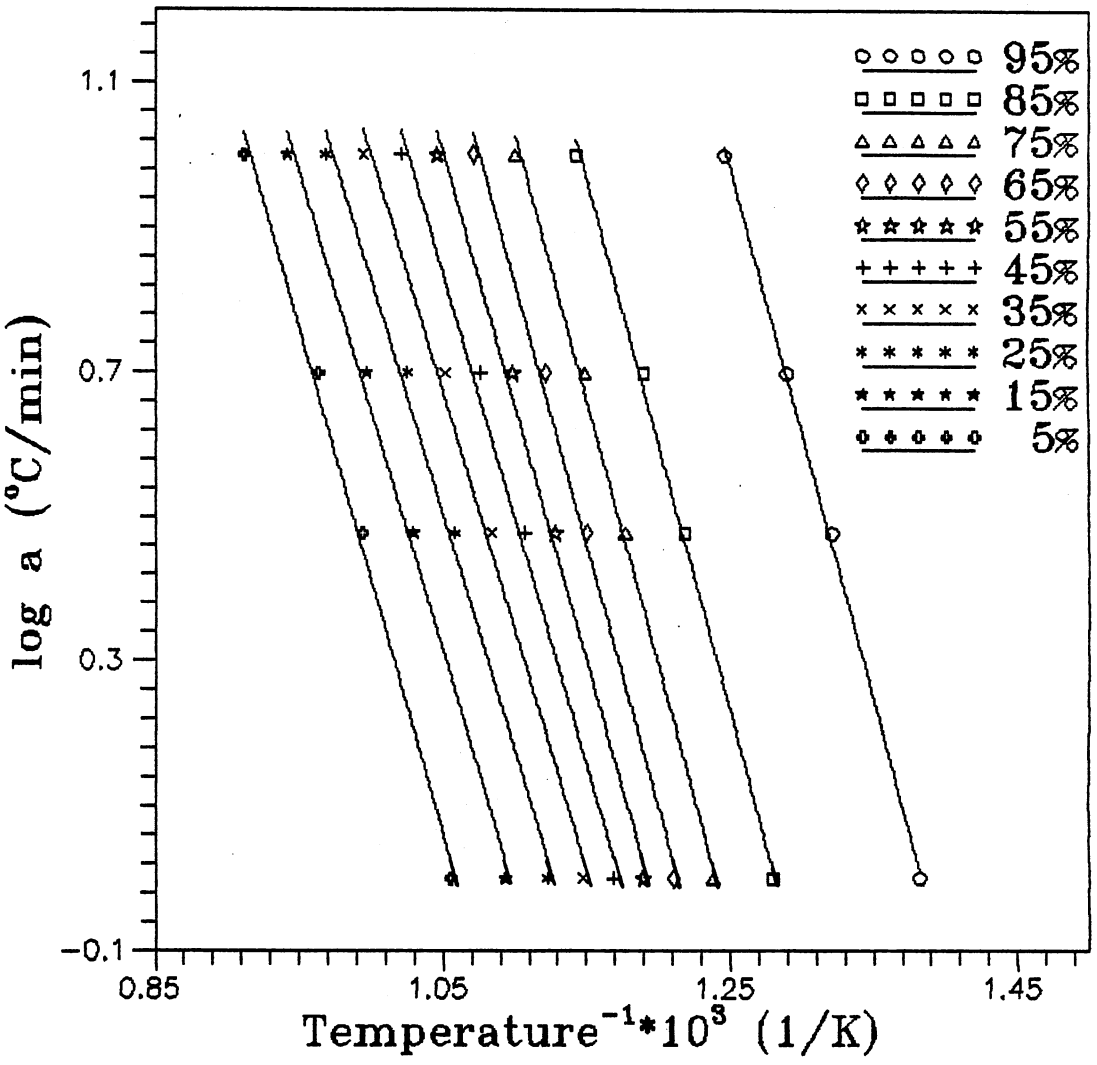

Figure 12. Plots of Logarithmic Heating Rate Against the Reciprocal Absolute Temperature for Different Conversions of the Decomposition of Emeraldine Base

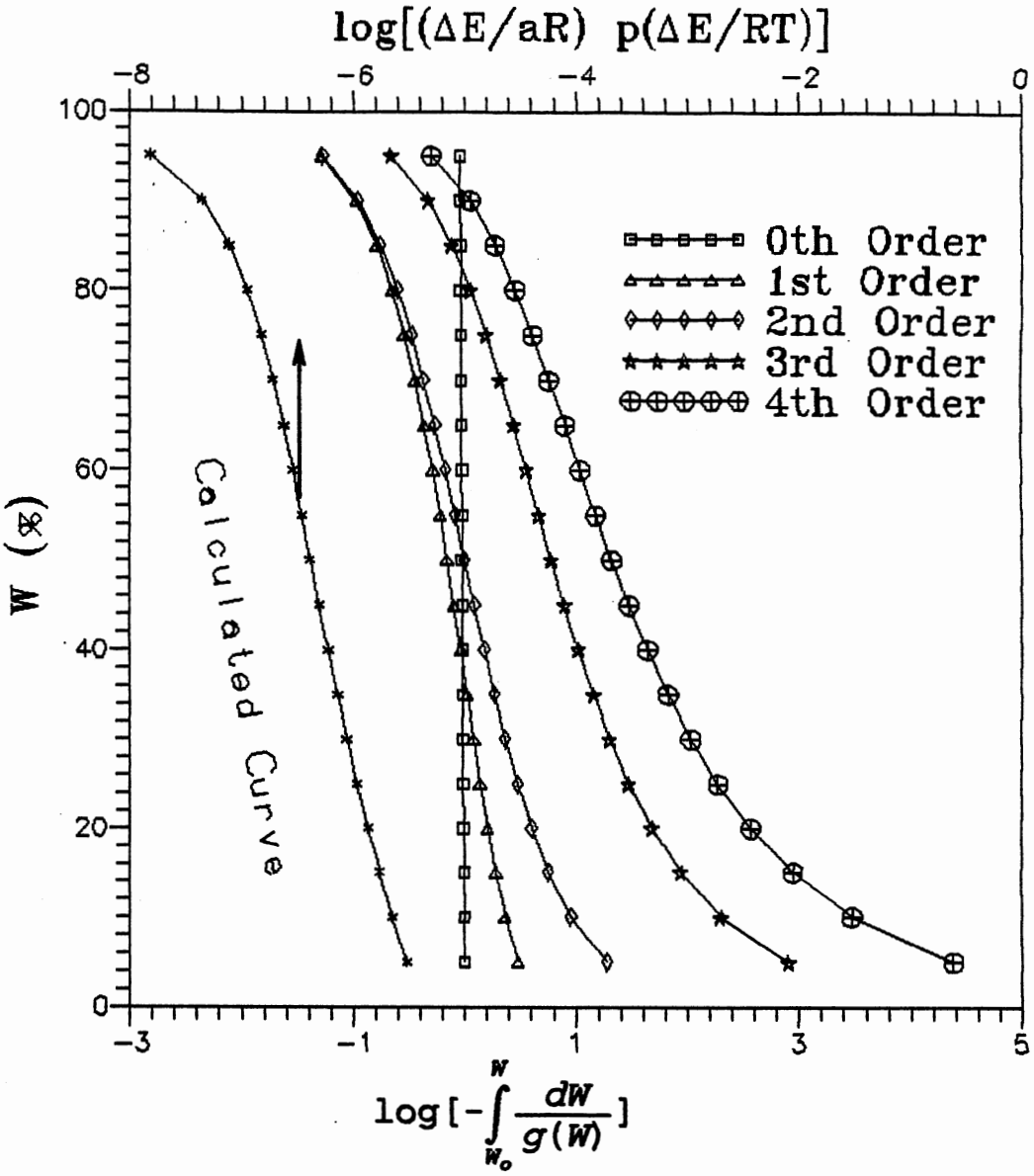

Figure 13. Comparison of the Calculated Curve with Different Reaction Orders for Emeraldine Base

TABLE VII

KINETIC PARAMETERS OF THE DECOMPOSITION OF EMERALDINE BASE

W	Slope	ΔE	log A
0.95	-7.399	32189.2	6.5420
0.90	-7.385	32129.2	6.4009
0.85	-7.398	32188.9	6.3551
0.80	-7.385	32130.9	6.3420
0.75	-7.360	32020.8	6.3411
0.70	-7.309	31800.4	6.3475
0.65	-7.240	31500.0	6.3568
0.60	-7.149	31104.0	6.3670
0.55	-7.036	30613.9	6.3773
0.50	-6.912	30071.8	6.3869
0.45	-6.785	29519.9	6.3952
0.40	-6.673	29033.1	6.4029
0.35	-6.585	28648.9	6.4117
0.30	-6.529	28407.4	6.4228
0.25	-6.518	28359.4	6.4398
0.20	-6.561	28544.7	6.4684
0.15	-6.649	28926.3	6.5180
0.10	-6.790	29542.7	6.6084
0.05	-7.020	30540.6	6.8050
mean		30382.8	6.4362
		A	2.73×10^6

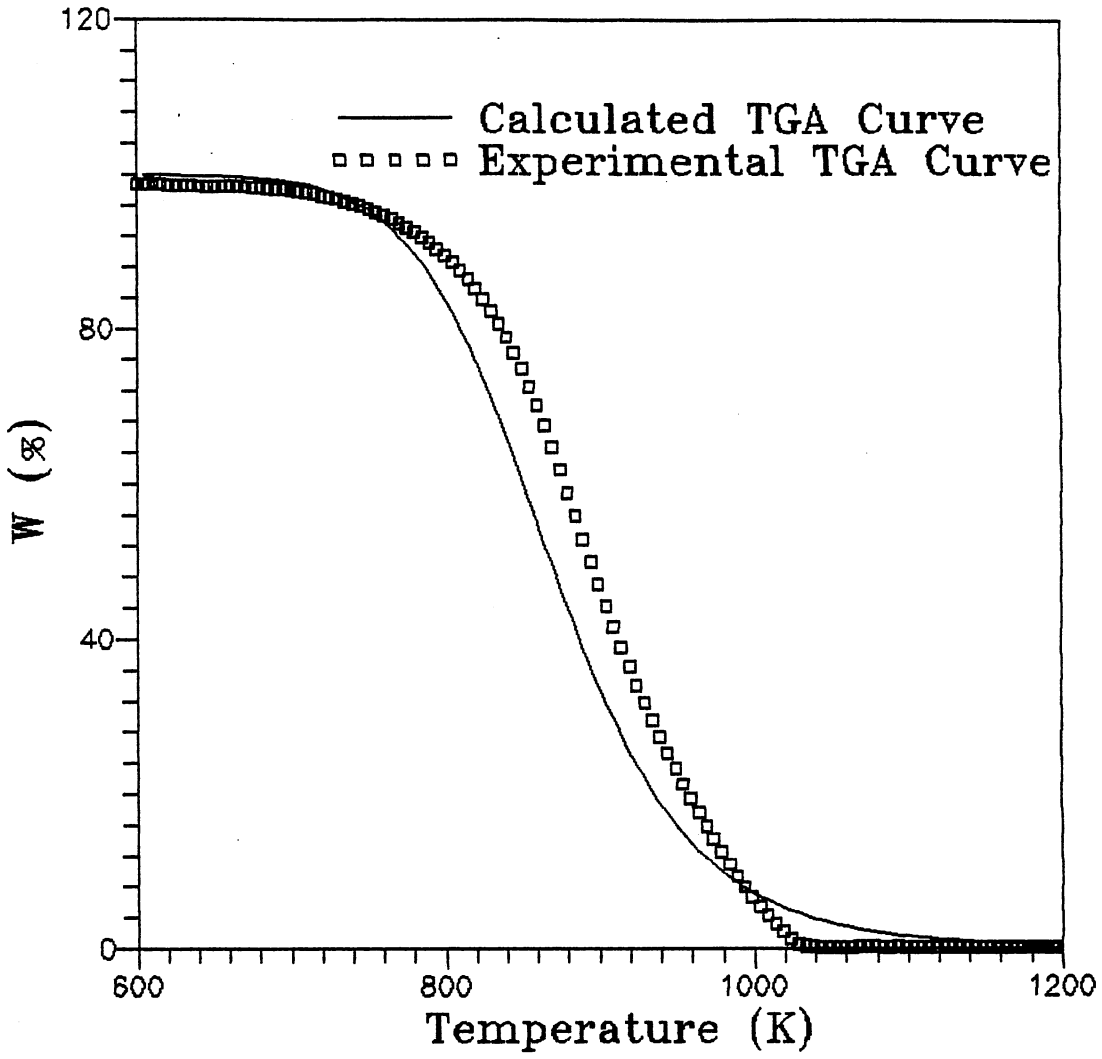

Figure 14. Comparison of Experimental and Calculated TGA Curves of Emeraldine Base at a Heating Rate of 3°C/min

$\Delta E/RT$ value was approximately 13 when the temperature approached 925°C. Then the Doyle's approximation was extended to the high temperature region to give a new approximation of:

$$\log(p(\frac{\Delta E}{RT})) = -1.5693-0.48813(\frac{\Delta E}{RT}) \quad . \qquad (13)$$

The plot of $\Delta E/RT$ versus $p(\Delta E/RT)$ is shown in Figure 15. The new approximation was used to calculate the activation energy and pre-exponential factor which were 30.9 kcal/mole and 1.91×10^6 min^{-1} respectively. The theoretical calculation used this set of parameters to get a much better fit of the experimental data, except at lower weight fraction which may cause by changing reaction order of degradation to one, as shown in Figure 16.

Sulfonated emeraldine thermodegradation was carried out under the same conditions as the emeraldine base. There were two major weight losses in the TGA curves of sulfonated emeraldine, as shown in Figures 17. The first major weight loss, before 600°C, was attributed to the release of sulfonic group (32), and the second major weight loss to chain scission. The detail used calculation graphs can refer to Figure 18. The kinetic parameters of the first weight loss were 4th order reaction, ΔE = 47.3 kcal/mole, and A = 2.9×10^{20} min^{-1}. For the second weight loss: 3rd order reaction, ΔE = 32.1 kcal/mole, and A = 3.6×10^7 min^{-1}, as shown in Table VIII. A discussion of these higher

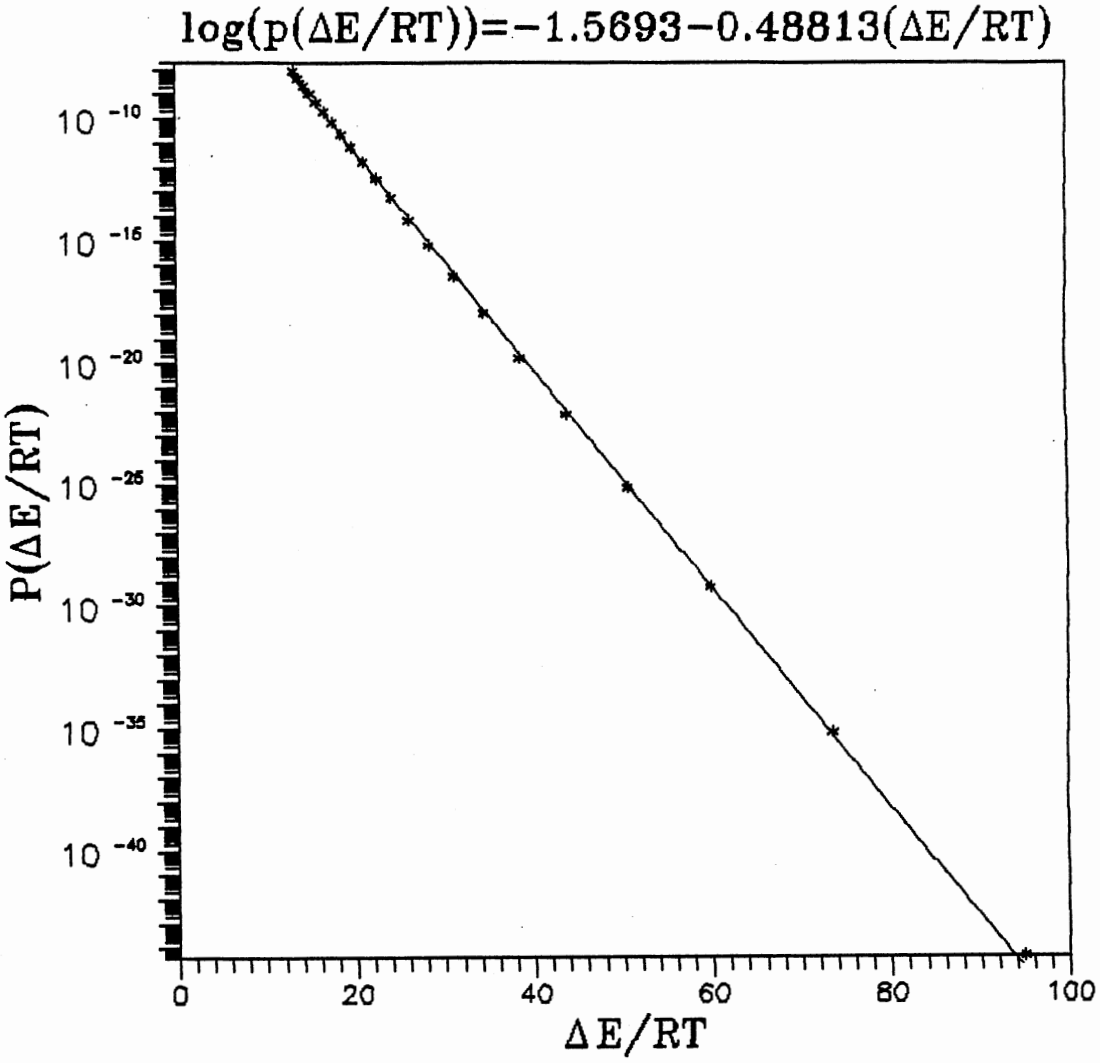

Figure 15. Doyle's Intergral Term

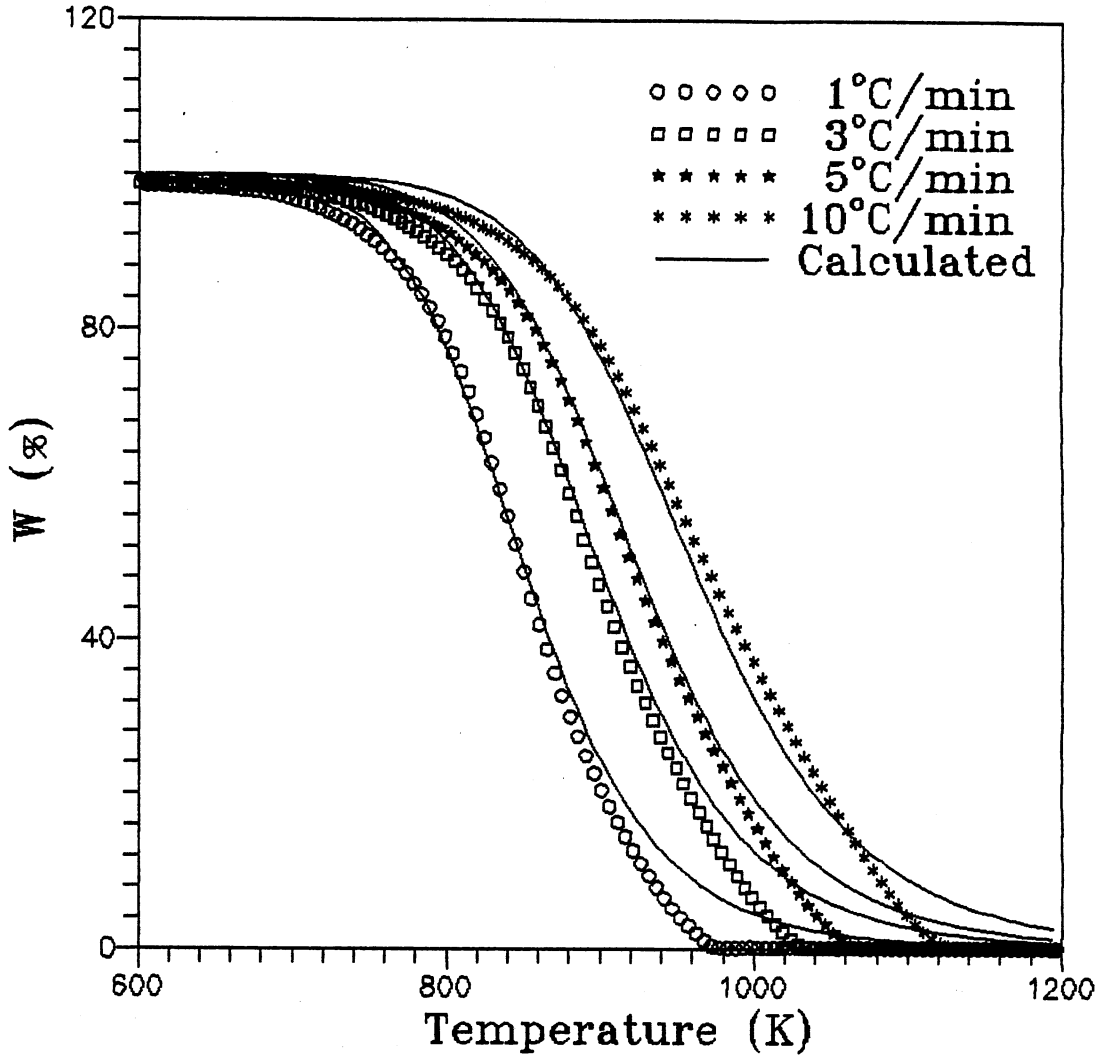

Figure 16. Comparison of Experimental and Calculated TGA Curves of Emeraldine Base

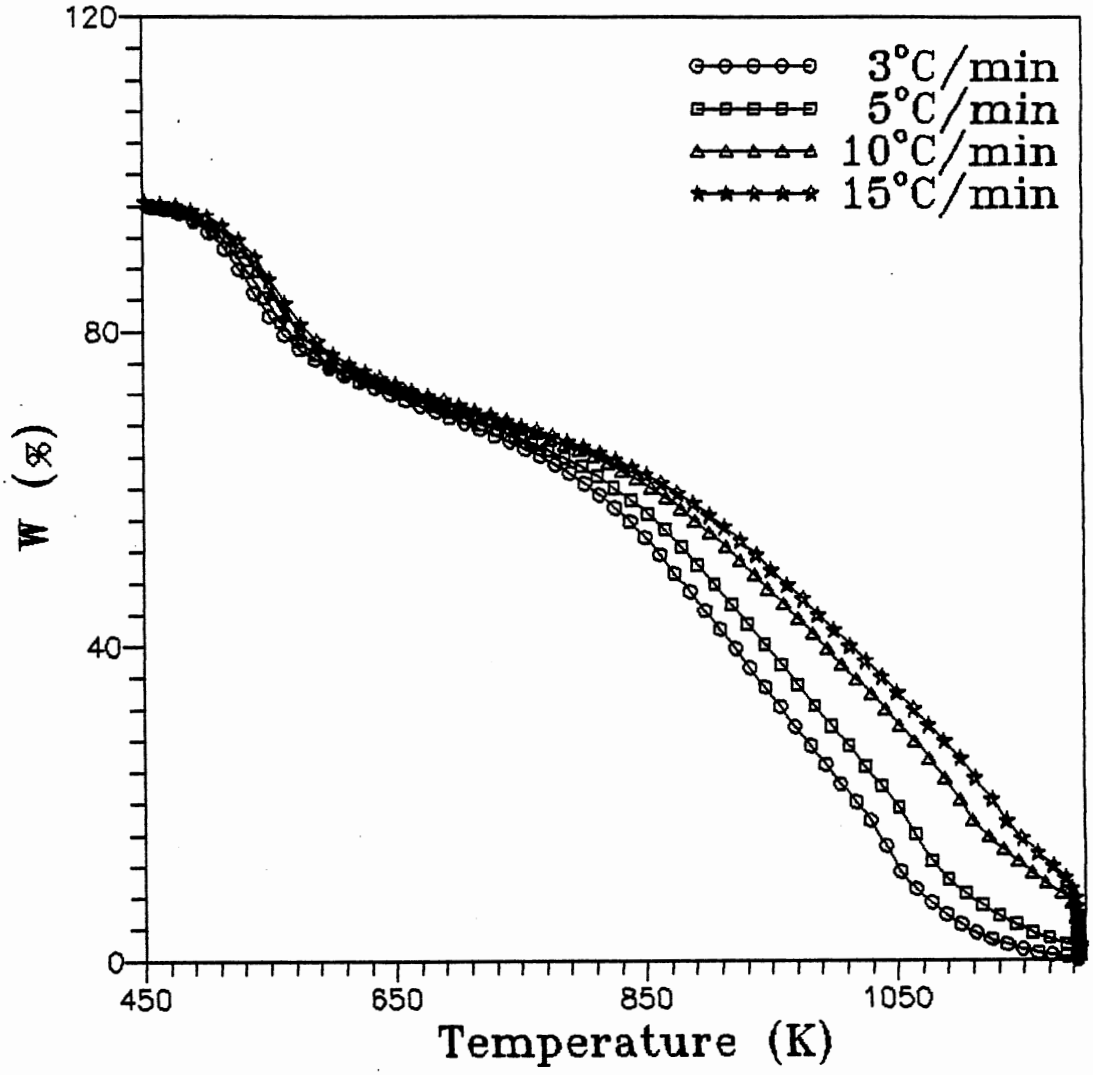

Figure 17. TGA Curves of Sulfonated Emeraldine at Various Heating Rates

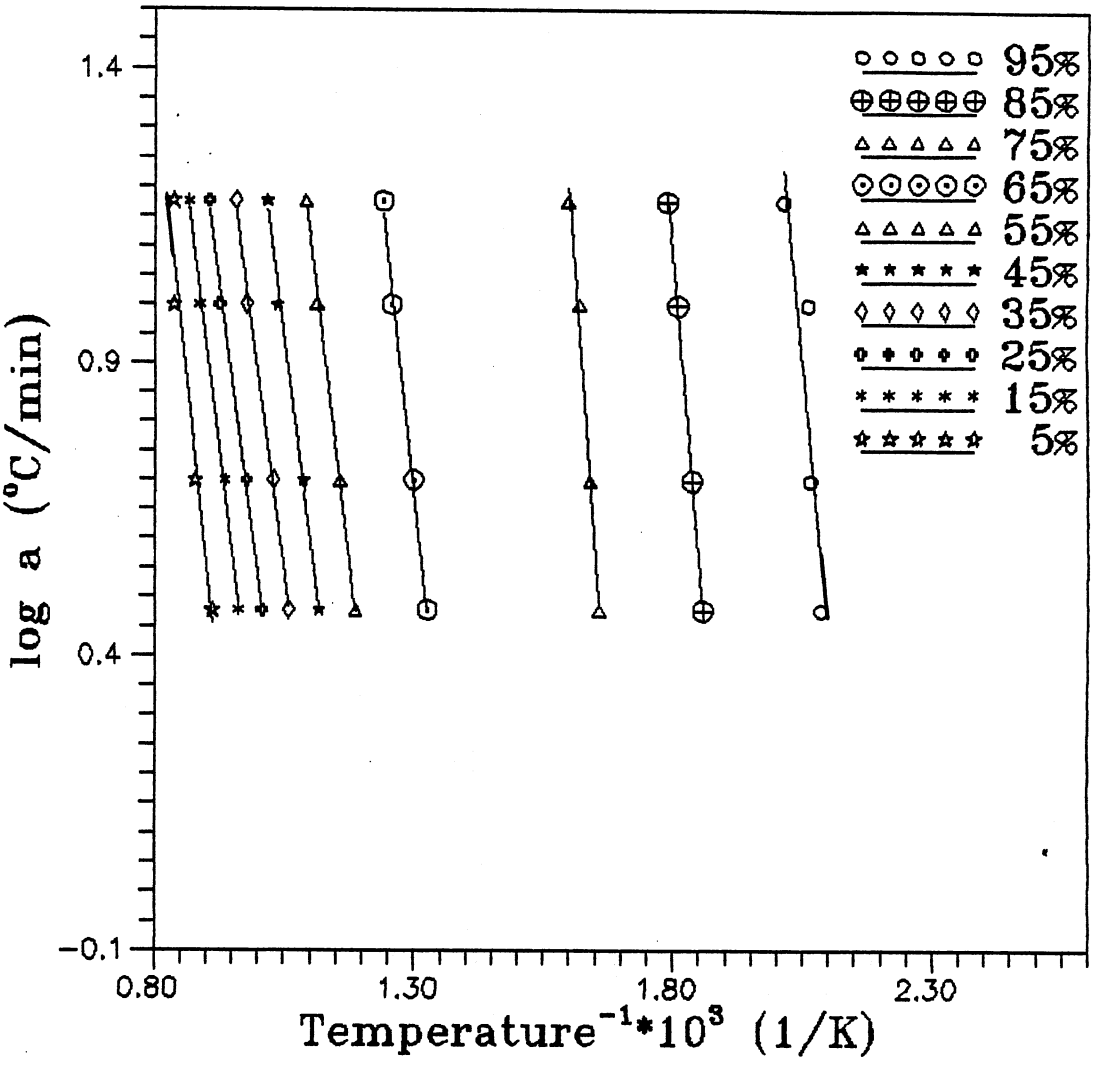

Figure 18. Plots of Logarithmic Heating Rate Against the Reciprocal Absolute Temperature for Different Conversions of the Decomposition Sulfonated Emeraldine

TABLE VIII

KINETIC PARAMETERS OF THE DECOMPOSITION OF EMERALDINE BASE

W	Slope	ΔE	log A
0.95	-9.367	40752.9	21.5162
0.90	-10.813	47044.5	20.3553
0.85	-10.578	46023.8	20.0801
0.80	-11.151	48513.8	20.0369
0.75	-12.408	53984.4	20.3425
mean		47263.9	20.4662
		A	2.9×10^{20}
0.70	-9.910	43117.2	8.7976
0.65	-8.112	35294.1	8.1173
0.60	-7.681	33418.6	7.7226
0.55	-7.446	32397.6	7.5329
0.50	-7.254	31561.9	7.4196
0.45	-6.966	30307.3	7.3292
0.40	-6.842	29768.9	7.2560
0.35	-6.677	29051.5	7.2031
0.30	-6.600	28717.0	7.1738
0.25	-6.687	29094.7	7.1734
0.20	-7.217	31401.4	7.2269
0.15	-7.128	31011.9	7.3488
0.10	-6.469	28147.2	7.5353
0.05	-8.450	36764.4	7.9756
mean		32146.7	7.5580
		A	3.61×10^{7}

reaction orders is given in Appendix B. These parameters were used to plot the residue weight against temperature, as shown in Figure 19. The calculated data do not fit the experimental data well. The integral method always assumes that only one reaction order takes place throughout the whole process. Comparing the TGA curves of emeraldine base and sulfonated emeraldine, the shape of sulfonated emeraldine was not as smooth as emeraldine base. Obviously, the reaction order changed during the degradation process. It is difficult to analyze the reaction transition by Doyle's method. This phenomenon promotes the difficulty in predicting the material lifetime, since the low temperature reaction is different than the high temperature reaction. However, these results may be used to predict the temperature contribution for the thermodegradation reaction in air environment.

In addition to the Ozawa method, two differential methods (Anderson and Freeman (46) and Freeman and Carroll (47)); and one integral method (MacCallum and Tanner (48)) were investigated. The differential methods required greater precision that allowed by the A/D board for satisfactory results. The Anderson and Freeman method requires an extrapolation $\Delta\log(dw/dt)$ as a function of $\Delta\log W_r$ curve to $\Delta\log W_r = 0$ in order to determine the activation energy. This method produced inconsistent and unreproduceable results due to the limited precision of the A/D board. Similar difficulties were encounter with the Freeman and Carroll method.

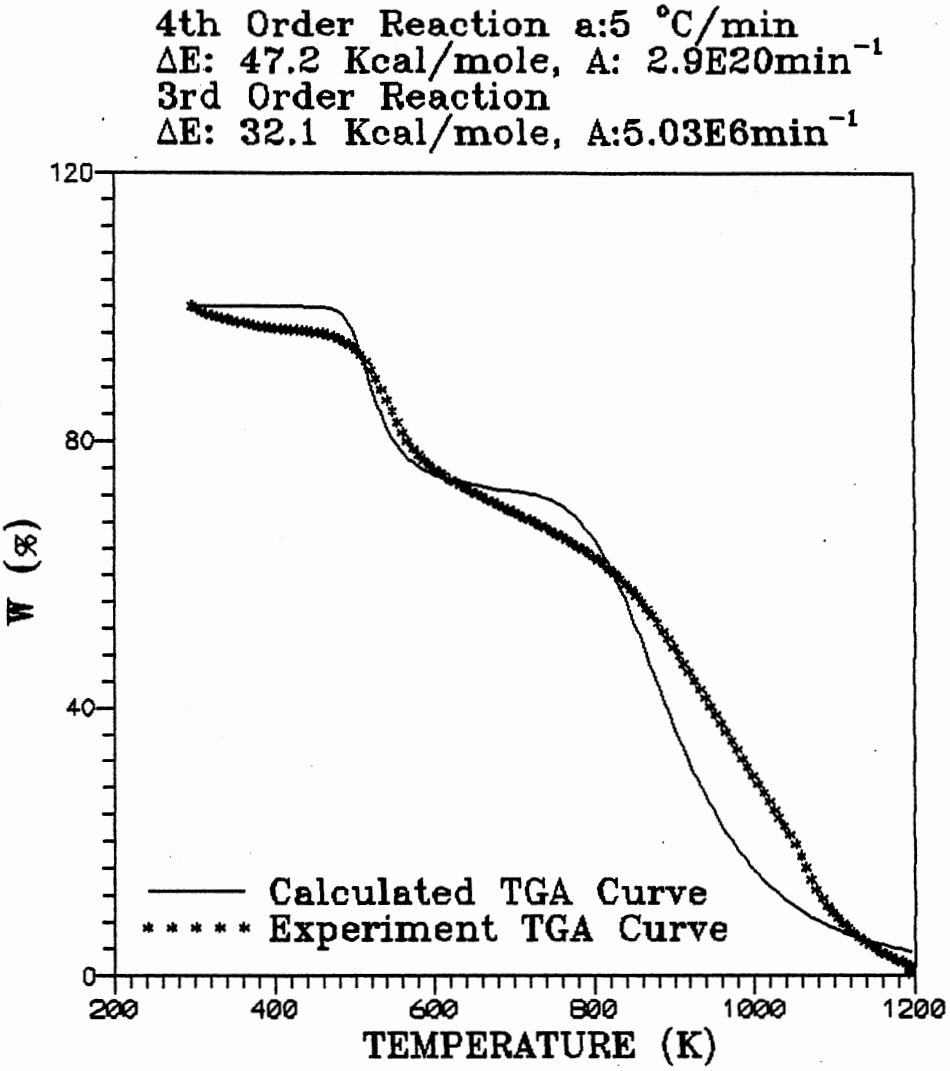

Figure 19. Comparison of Experimental and Calculated TGA Curves of Sulfonated Emeraldine

The integral method of MacCallum and Tanner produced results consistent with the Ozawa method. However, the trial and error nature of the MacCallum and Tanner method made it more cumbersome and time consuming than the Ozawa method. Hence the Ozawa method was selected.

There are two possible ways to explain the two major weight losses in TGA curve for sulfonated emeraldine. Yue et al. (32) proposed that the first major weight loss could be attributed to the release of the sulfonic acid groups and the second major weight loss to the main chain scission. This mechanism is similar to the degradation mechanism of hydrochloride emeraldine (17). Alternatively, it has been proposed that the sulfonated samples actually consisted two distinct materials. We believed that the material under study was the same as Yue et al. (40), since the same procedure was followed and the resultant material shows the same color and electrically conductivity as reported by Yue et al. Yue et al. showed by FTIR that the SO_3^- groups were attached to the aromatic ring. However, there was no evidence to believe that only one SO_3^- group was attached to each aromatic ring, leading to the possibility that a second sulfonation resulted in a second material. Yue et al. (32) proposed that the increased thermostability of sulfonated emeraldine during the second major weight loss could be attributed to covalently bonded sulfonic groups on the emeraldine chain. Evidence for either mechanism is inconclusive. However, the issue could be settled by a modification of the GC to detect sulfonic acid.

Thermodegradation Products

The thermodegradation of emeraldine base and sulfonated emeraldine was carried out in an helium environment at atmosphere pressure, and the degradation products were purged to GC for analysis. The TGA curves are shown in Figures 20 and 21. Hydrogen and methane were the only degradation products identified by GC. The concentrations of the degradation products at different temperature are shown in Tables IX and X. There was no gas degradation component observed during the major weight loss, as shown in Figures 20 and 21. Since the GC columns were chosen to separate the gas degradation components and flush out the heavy components, the high boiling point degradation products like aniline, p-phenylenediamine, n-phenylaniline, and N-phenyl-1,4-benzenediamine, as identified by Traore et al. (39) in Figure 3, were not observed. However, condensed reddish yellow particles were observed on the relatively cold hangdown tube wall above the furnace. From Tables IX and X, the mass of hydrogen and methane released from the samples were estimated to be 0.1202 mg and 0.1553 mg for emeraldine base and sulfonated emeraldine, respectively. The hydrogen and methane mass were relatively small compared to the 34.0 mg and 46.6 mg weight loss for emeraldine base and sulfonated emeraldine, respectively. Therefore, most of the degradation products which were not identified by GC deposited on the cold hangdown tube wall. After the major weight loss, hydrogen and methane were observed. The

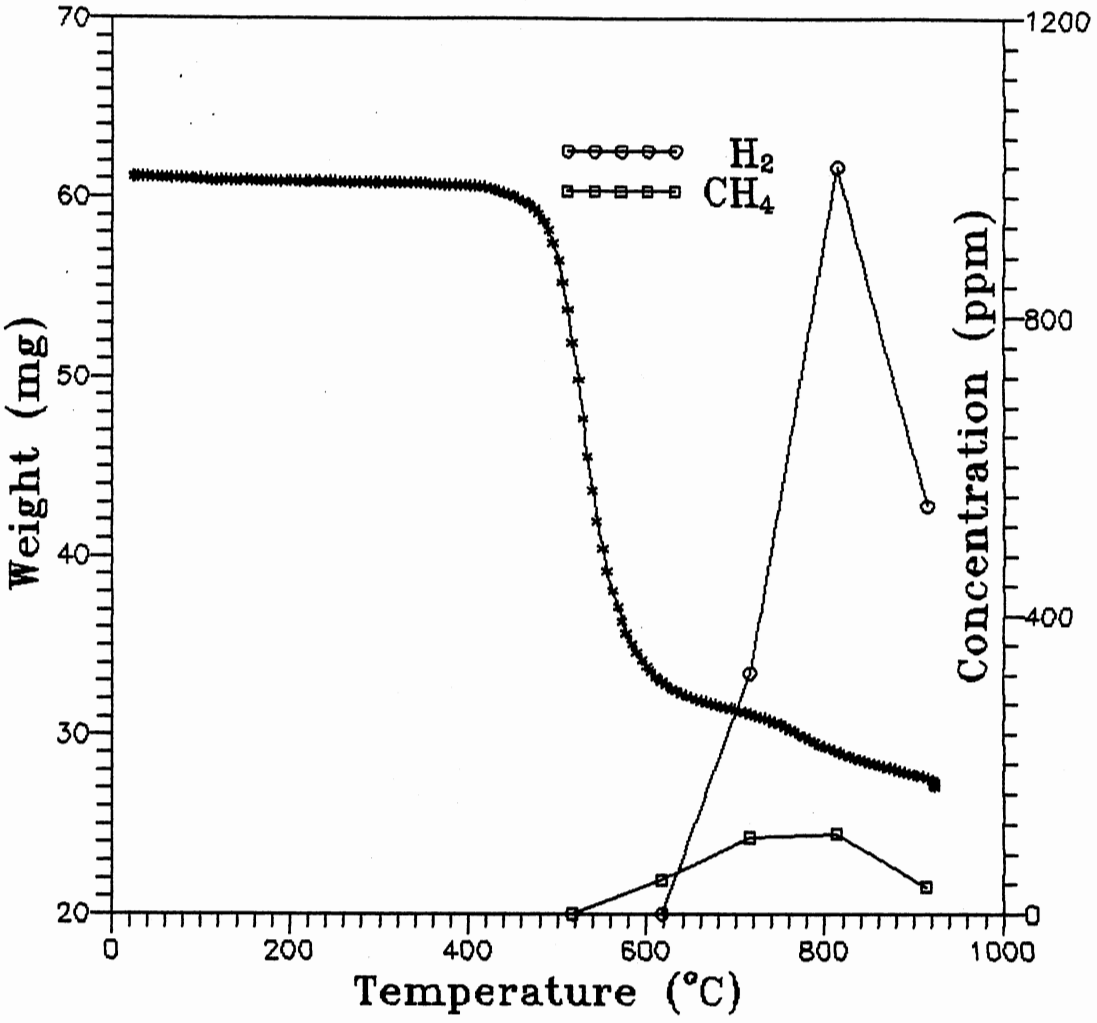

Figure 20. TGA Curve and Degradation Products Concentration of Emeraldine Base at a Constant Heating Rate 6.67°C/min in Helium Environment

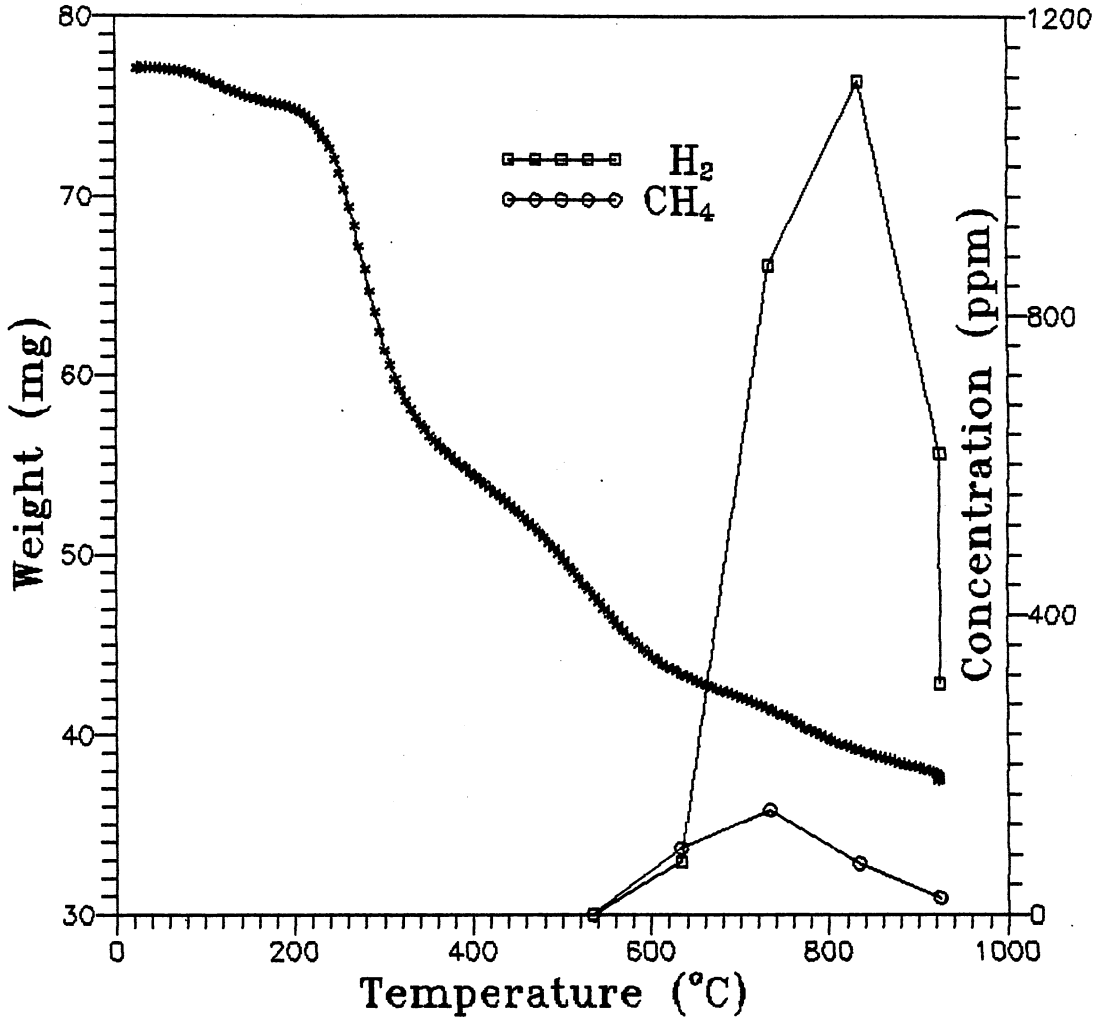

Figure 21. TGA Curve and Degradation Products Concentration of Sulfonated Emeraldine at a Heating Rate 6.67°C/min in Helium Environment

TABLE IX

THERMODEGRADATION PRODUCTS OF EMERALDINE BASE

Temperature(°C)	Hydrogen, ppm	Methane, ppm
617	0.0	45.8
716	322.4	102.4
814	1000.3	107.3
914	548.0	36.9

* Purge gas flow rate = 25.5 ml/min

TABLE X

THERMODEGRADATION PRODUCTS OF SULFONATED EMERALDINE

Temperature(°C)	Hydrogen, ppm	Methane, ppm	CO, ppm
535	0.0	0.0	310.8
634	70.2	87.5	306.8
733	868.2	138.8	292.8
833	1114.3	68.0	396.0
924	614.9	22.7	486.7
20 min. after 925	308.2	22.4	487.7

* Purge gas flow rate = 27 ml/min

hydrogen component was released from the reduced repeating unit in emeraldine base as the chain fused to ladder structure of carbazole group, as proposed by Traore et al. in Figure 3. This was supported by the degradation residues high electric conductivity, which was similar to the pyrolysis product of polyacrylonitrile (carbon fiber) as shown in Figure 22. However, this still needs further study by nuclear magnetic resonance (NMR) spectroscopy. The methane component came from the oxidized mer. According to Traore et al. study, it was proposed that the methane should be accompanied by ammonia and acetylene. This may show the different degradation mechanisms between vacuum and helium environment.

Referring to the mechanism in Figure 3, the reduced mers decompose to ammonia, aniline, p-phenylenediamine, N-phenylaniline, and N-phenyl-1,4-benzenediamine. However, the higher boiling point components were not identified by the GC because the column had been selected to analyze these low boiling point molecules. From the mass balance discussed above, the high boiling point degradation products could have cause the bulk of the weight loss. The possible reason for not identified ammonia is that the ammonia may not easily escape from the decomposed oligomer which deposited on hangdown tube in helium environment. Degradation of the reduced mers at high temperatures is consistent with the detection of hydrogen as is shown in Figure 22. The Traore et al. proposed mechanism for the

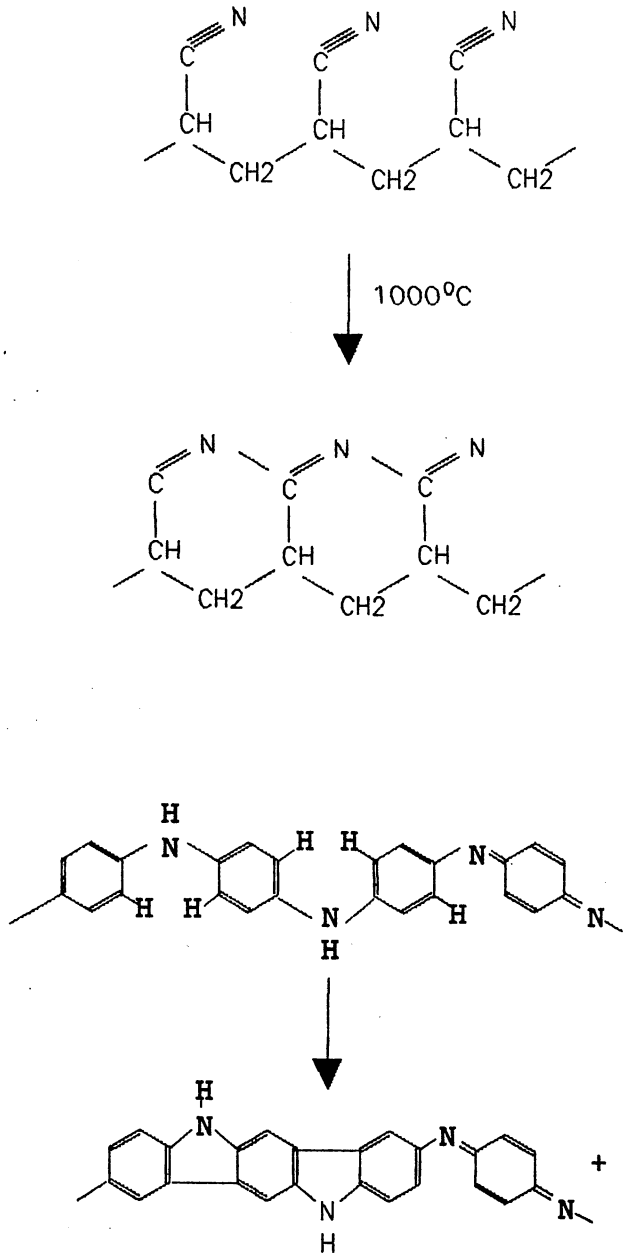

Figure 22. The Pyrolysis Products of Polyacrylonitrile and Proposed Pyrolysis Products of Polyaniline

degradation of oxidized mers results in production of ammonia, acetylene, and methane. However, only methane was identified leading to the conclusion that there may be another degradation mechanism. The pyridine-based heterocycle degradation product from the other oxidized mer degradation mechanism can only be detected by IR.

CHAPTER V

CONCLUSIONS AND RECOMMENDATIONS

Several conclusions can be made from the results of this study. These conclusions are:

1. The kinetic parameters of emeraldine base are as follows:

   Reaction Order: 2nd Order

   Activation energy, ΔE: 30.9 kcal/mole

   Pre-exponential factor, A: 1.91×10^{6} min^{-1}

   The kinetic parameters of sulfonated emeraldine are as following:

   First major weight loss

   Reaction Order: 4th Order

   Activation energy ΔE: 47.3 kcal/mole

   Pre-exponential factor (A): 2.9×10^{20} min^{-1}

   Second major weight loss

   Reaction Order: 3rd Order

   Activation energy, ΔE: 32.1 kcal/mole

   Pre-exponential factor, A: 3.61×10^{7} min^{-1}

2. Hydrogen and methane were the only degradation products identified by the GC among the possibilities of hydrogen, methane, ammonia, acetylene, carbon monoxide, and carbon dioxide.

Several observations were made during this experimental

study and the following recommendations are made:

1. Although the Ozawa integration method can obtain more accurate kinetic parameters than other methods, only one decomposition reaction mechanism was assumed throughout the entire process. The differential method may be used for detail investigation during the decomposition process, especially for sulfonated emeraldine which involves the reaction transition at different stages of the weight loss.

2. Pyrolysis GC should be used to eliminate the effect of the secondary reaction, resulting from the reaction on the hot hangdown tube wall.

3. The degradation residue needs further investigation by NMR to reveal the degradation mechanism.

4. The high boiling point degradation products which cause the major weight loss need further analysis to reveal the degradation mechanism.

BIBLIOGRAPHY

(1) MacDiarmid, A. G., Chiang, J.-C. & Halpern, M. et al. American Chemical Society. Division of Polymer Chemistry. Polymer Preprints 25, 248-249 (1984).

(2) Caja, J., Kaner, R. B. & MacDiarmid, A. G. Journal of the Electrochemical Society 131, 2744 (1984).

(3) Maxfield, M., Mu, S. L. & MacDiarmid, A. G. Journal of the Electrochemical Society 132, 838-841 (1985).

(4) Kitani, A., Kaya, M. & Sasaki, K. Journal of the Electrochemical Society 133, 1069-1073 (1986).

(5) MacDiarmid, A. G., Mu, S.-L. & Somasiri, N. L. D. Mol. Cryst. Liq. Cryst. 121, 187-190 (1985).

(6) MacDiarmid, A. G., Yang, L. S. & Huang, W. S. et al. Synthetic Metals 18, 393-398 (1987).

(7) Mengoli, G., Musiani, M. M. & Pletcher, D. et al. Journal of the Applied Electrochemistry 17, 515-531 (1987).

(8) Osaka, T., Ogano, S. & Naoi, K. Journal of the Electrochemical Society 136, 306-309 (1989).

(9) Scrosati, B. Journal of the Electrochemical Society 136, 2774-2782 (1989).

(10) McManus, P. M., Cushman, R. J. & Yang, S. C. The Journal of Physical Chemistry 91, 744-747 (1987).

(11) Kobayashi, T., Yoneyama, H. & Tamura, H. Journal of Electroanalytical Chemistry 177, 293-297 (1984).

(12) Batich, C. D., Laitinen, H. A. & Zhou, H. C. Journal of the Electrochemical Society 137, 883-885 (1990).

(13) Kobayashi, T., Yoneyama, H. & Tamura, H. Journal of Electroanalytical Chemistry 161, 419-423 (1984).

(14) Chiang, C. K., Fincher, C. R. Jr. & Park, Y. W. et al. Physical Review Letters 39, 1098-1101 (1977).

(15) Green, A. G. & Woodhead, A. E. Journal of Chemical Society 97, 2388-2403 (1910).

(16) Epstein, A. J., Ginder, J. M. & Richter, A. F. et al. Conducting Polymer (Alcacer, L.) Dordrecht, Holland (D Reidel, 1987).

(17) Hagiwara, T., Yamaura, M. & Iwata, K. Synthetic Metals 25, 243-252 (1988).

(18) Mohilner, D. M. , Ralph N. Adams & William J. Argersinger, J. Journal of American Chemical Society 84, 3618-3622 (1962).

(19) Noufi, R., Nozik, A. J. & White, J. et al. Journal of the Electrochemical Society 129, 2261-2265 (1982).

(20) Oyama, N., Ohsaka, T. & Shimizu, T. Analytical Chemistry 57, 1526-1532 (1985).

(21) Paul, E. W., Ricco, A. J. & Wrighton, M. S. The Journal of Physical Chemistry 89, 1441-1447 (1985).

(22) Li, C., Wang, Y. & Wan, M. et al. Synthetic Metals 39, 91-96 (1990).

(23) Krinichniy, V. I., Eremenko, O. N. & Rukhman, G. G. et al. Synthetic Metals 41-43, 1137 (1991).

(24) Kost, K. M. & Bartak, D. E. Anal. Chem. 60, 2379-2384 (1988).

(25) Angelopoulos, M., Ray, A. & MacDiarmid, A. G. et al. Synthetic Metals 21, 21-30 (1987).

(26) MacDiarmid, A. G. & Arthur J. Epstein Faraday Discuss, Chem. Soc. 88, 317-332 (1989).

(27) Monkman, A. P. & Adams, P. Synthetic Metals 40, 87-96 (1991).

(28) Monkman, A. P. & Adams, P. Synthetic Metals 41-43, 627-633 (1991).

(29) Genies, E. M., Syed, A. A. & Tsintavis, C. Molecular Crystal and Liquid Crystal 121, 181-186 (1985).

(30) Travers, J. P., Chroboczek, J. & Devreux, F. et al. Mol. Cryst. Liq. Cryst. 121, 195-199 (1985).

(31) MacDiarmid, A. G., Chiang, J. R., A. F. & Somasiri, L. D. et al. Conducting Polymers (editor Alcacer, L.) 105-120 (D. Reidel, Dordrecht,Holland, 1987).

(32) Yue, J., Epstein, A. J. & Zhong, Z. et al. Synthetic Metals 41-43, 765-768 (1991).

(33) Green, A. G. & Woodhead, A. E. Journal of Chemical Society 101, 1117-1123 (1912).

(34) Hand, R. L. & Nelson, R. F. Journal of American Chemical Society 96, 850-860 (1974).

(35) Stilwell, D. E. & Park, S.-M. Journal of the Electrochemical Society 135, 2497-2502 (1988).

(36) Stilwell, D. E. & Park, S.-M. Journal of the Electrochemical Society 136, 688-698 (1989).

(37) LaCroix, J.-C. & Diaz, A. F. Journal of the Electrochemical Society 135, 1457-1463 (1988).

(38) Wei, Y. & Hsueh, K. F. Journal of Polymer Science: Part A: Polymer Chemistry 27, 4351-4363 (1989).

(39) Traore, M. K., Stevenson, W. T. K. & McCormick, J. et al. Synthetic Metals 40, 137-153 (1991).

(40) Yue, J. & Epstein, A. J. Journal of the American Chemical Society 112, 2800-2801 (1990).

(41) Flynn, J. H. & Wall, L. A. J. Res. Nat. Bur. Stand. 70A, 487 (1966).

(42) Ozawa, T. Chemical Society of Japan Bulletin 38, 1881-1886 (1965).

(43) Doyle, C. D. Journal of the Applied Polymer Science 5, 285-295 (1961).

(44) Madorskey, S. L. Journal of Polymer Science 9, 133-156 (1952).

(45) Oakes, W. G. & Richards, R. B. Journal of Chemical Society 2929 (1949).

(46) Anderson, D. A. & Freeman, E. S. Journal of Polymer Science 54, 253-260 (1961).

(47) Freeman, E. S. & Carroll, B. Journal of Physical Chemistry 62, 394-397 (1958).

(48) MacCallum, J. R. & Tanner, J. European Polymer Journal 6, 1033-1039 (1970).

APPENDIX A

RAW DATA

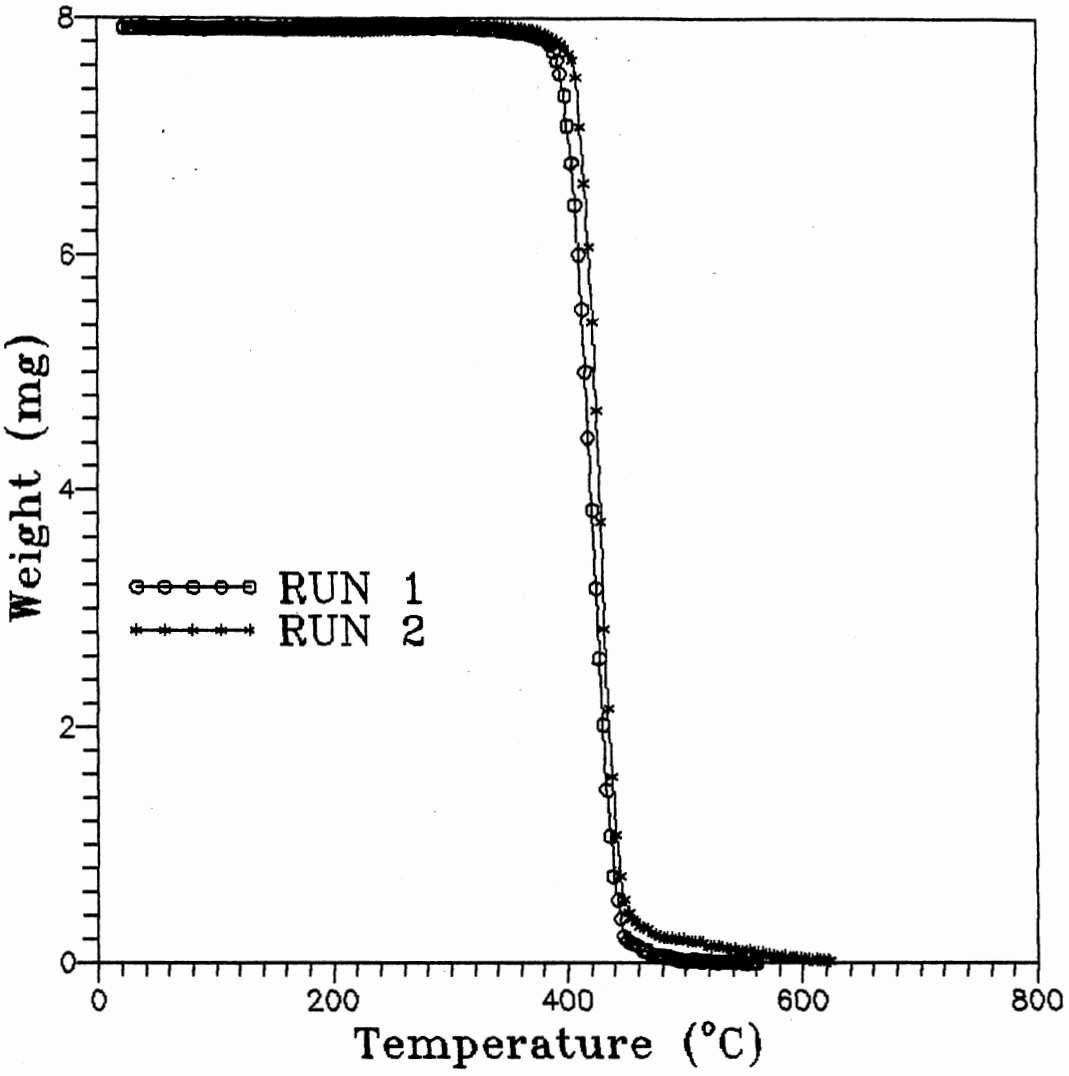

Figure 23. TGA Curves of Polyethylene at a Constant Heating Rate 1°C/min

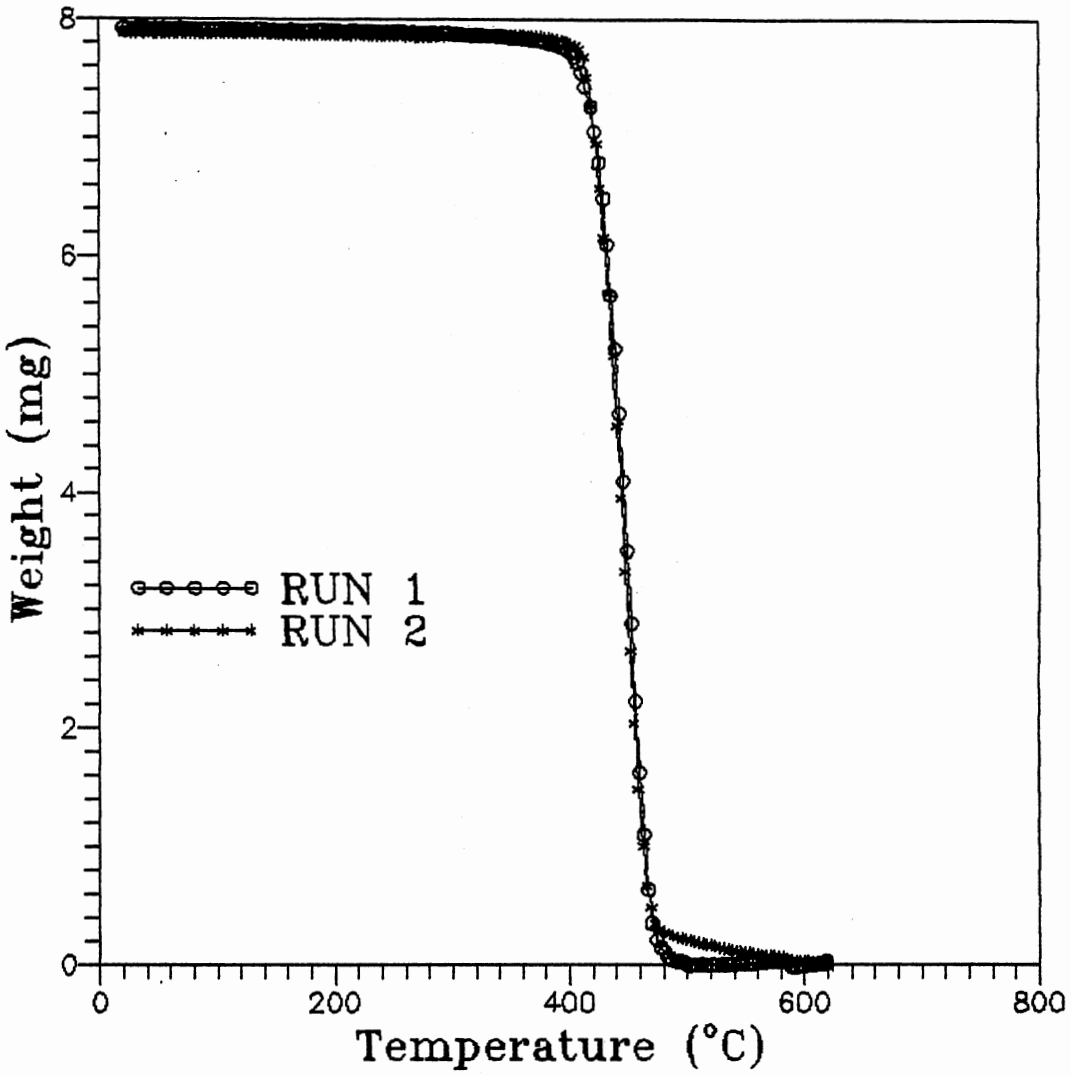

Figure 24. TGA Curves of Polyethylene at a Constant Heating Rate 3°C/min

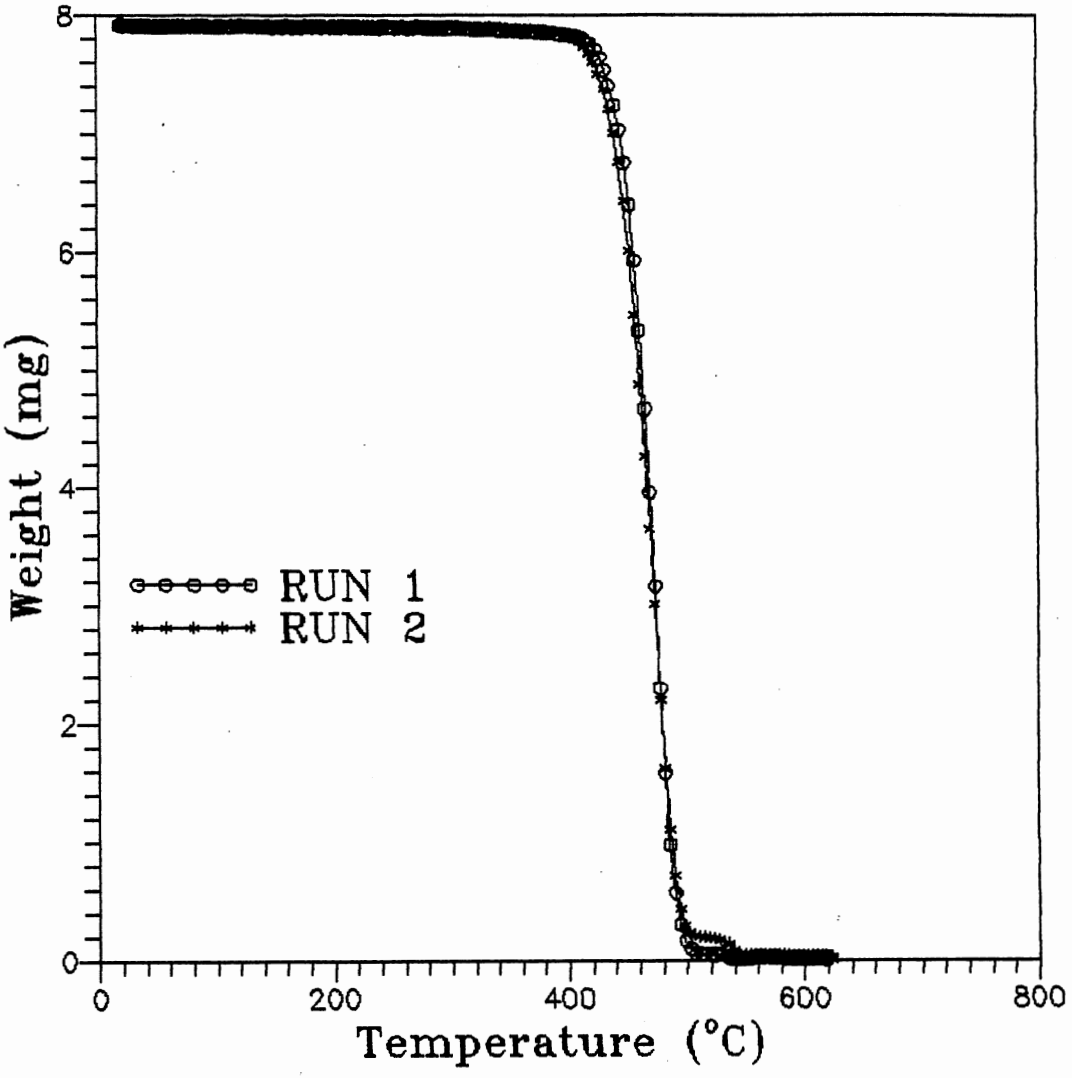

Figure 25. TGA Curves of Polyethylene at a Constant Heating Rate 5°C/min

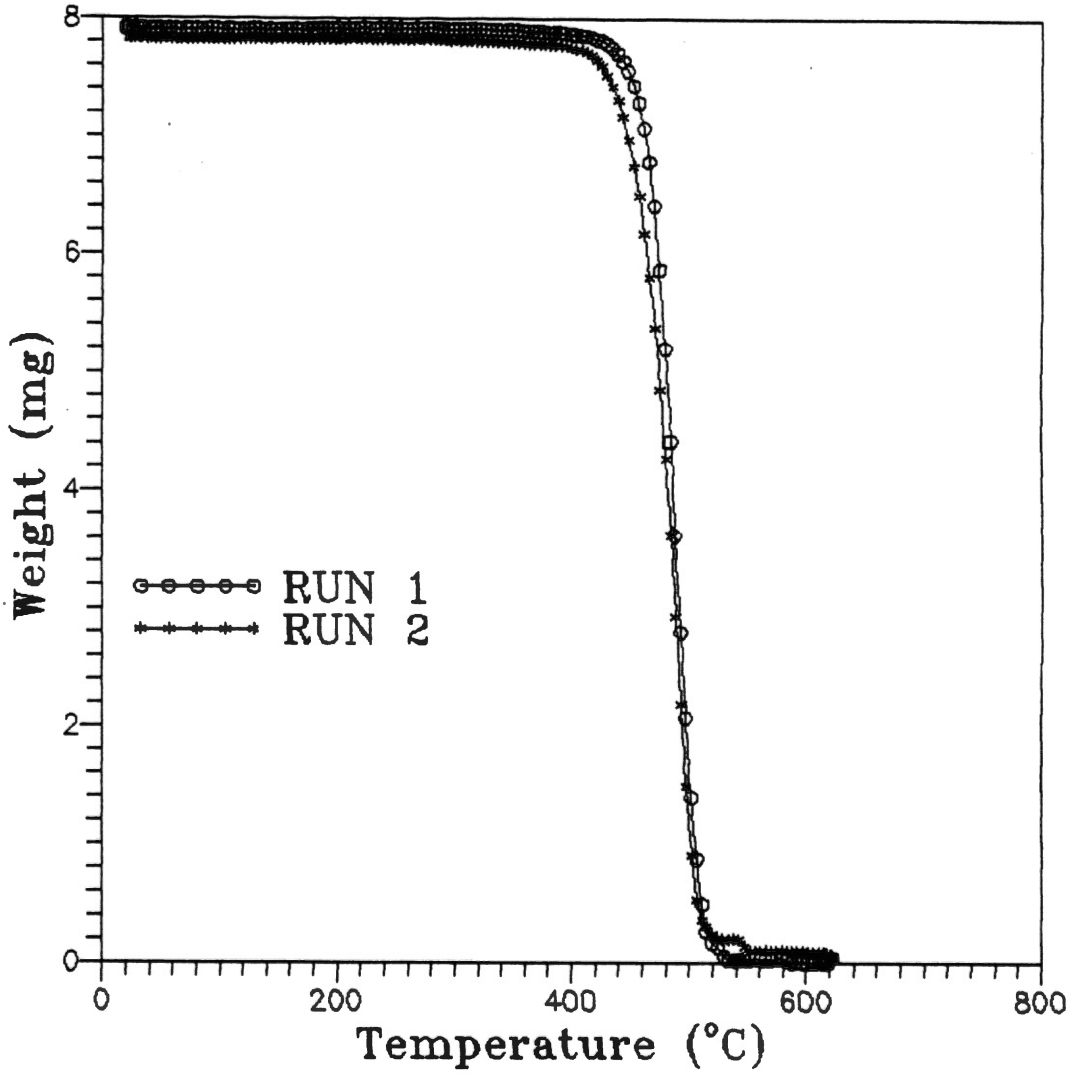

Figure 26. TGA Curves of Polyethylene at a Constant Heating Rate 10°C/min

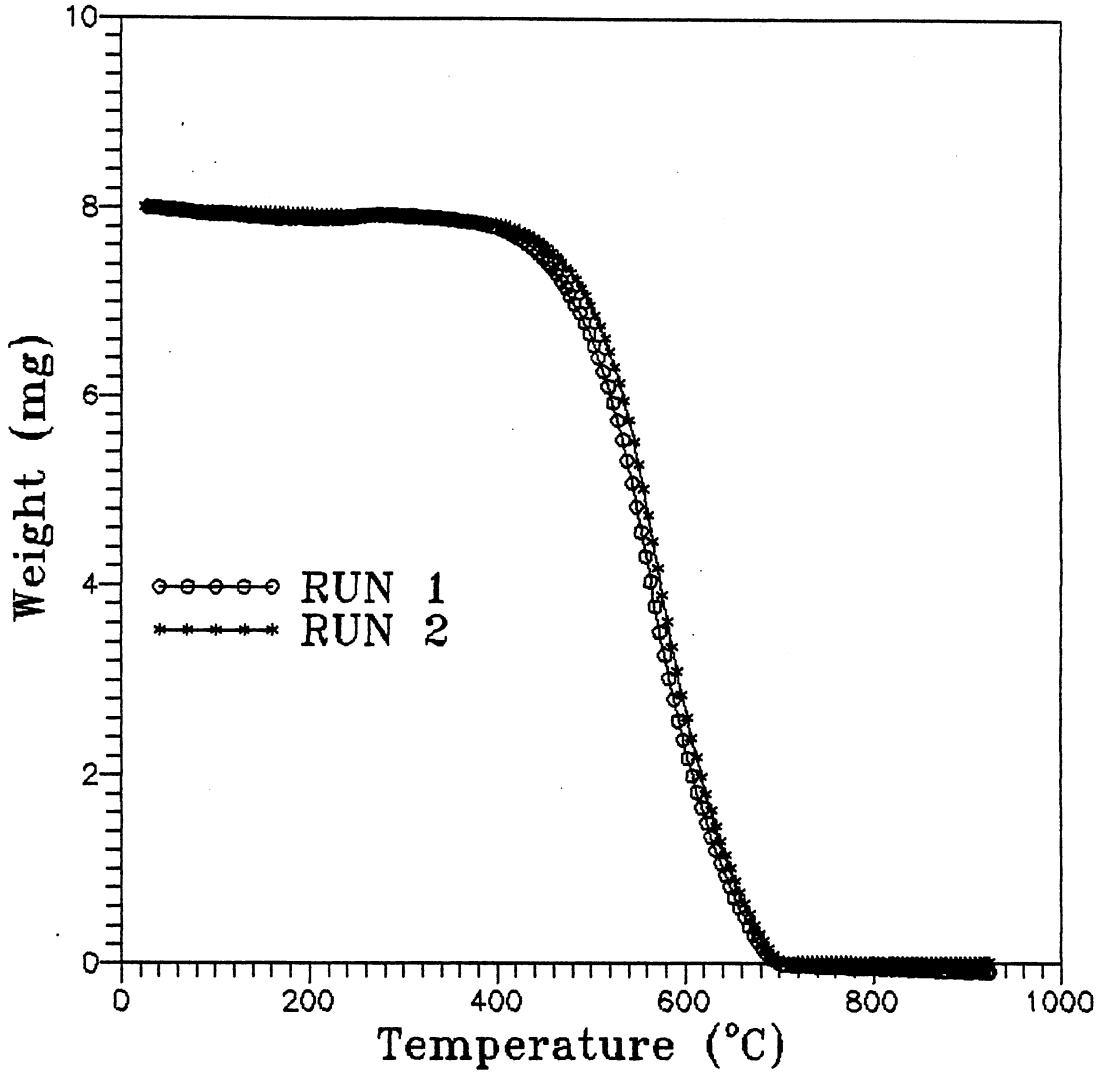

Figure 27. TGA Curves of Emeraldine Base at a Constant Heating Rate 1°C/min

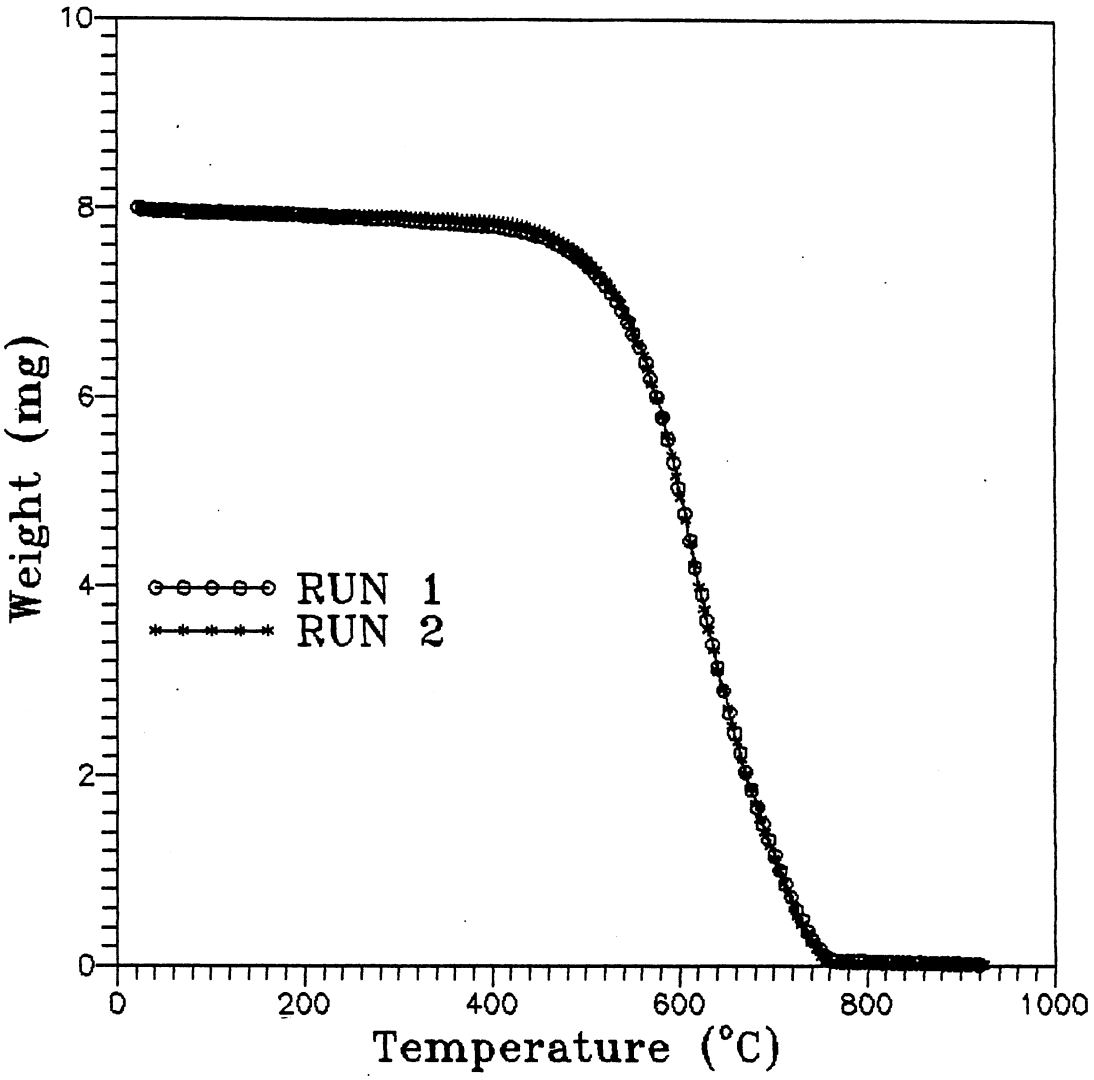

Figure 28. TGA Curves of Emeraldine Base at a Constant Heating Rate 3°C/min

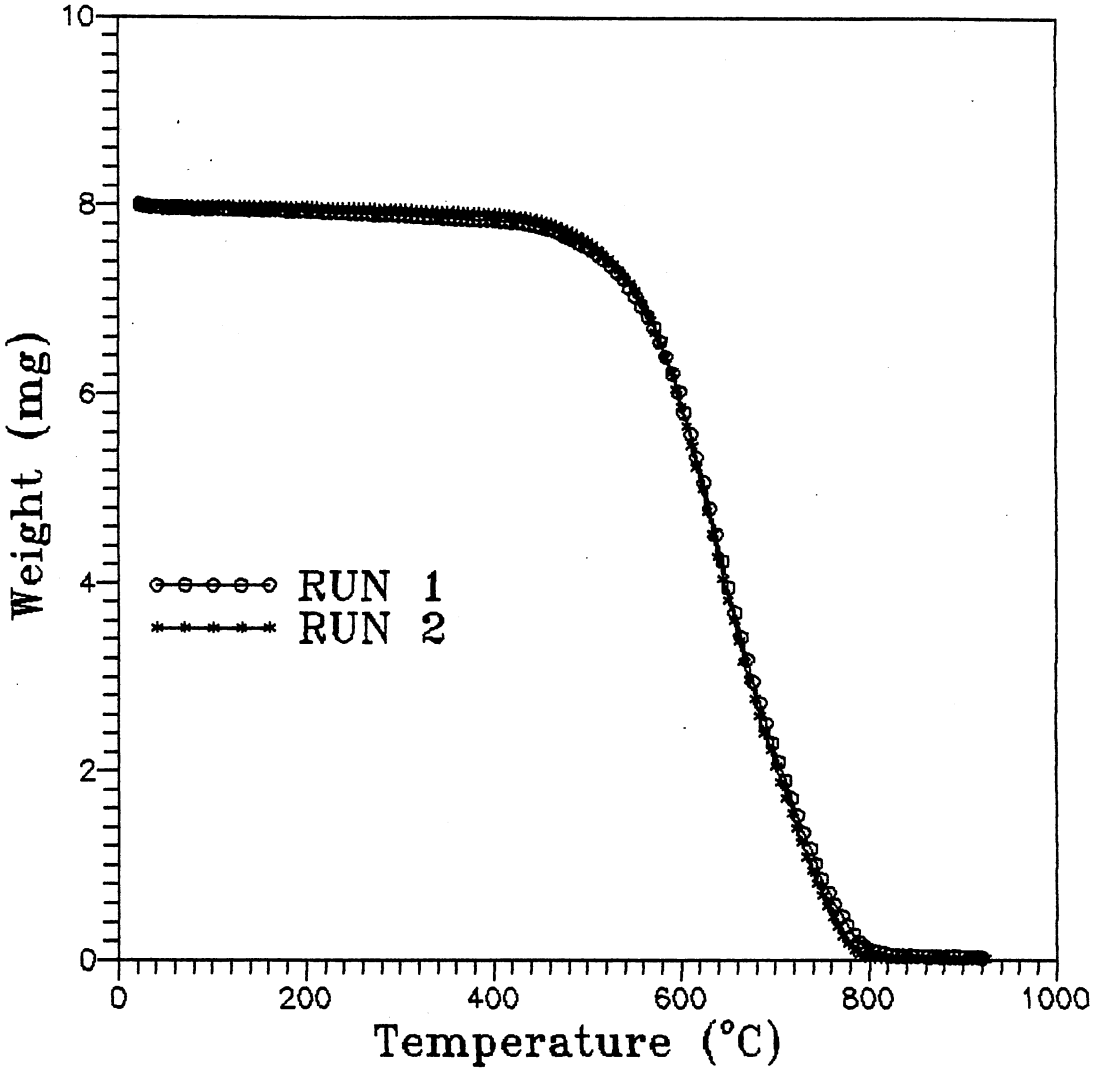

Figure 29. TGA Curves of Emeraldine Base at a Constant Heating Rate 5°C/min

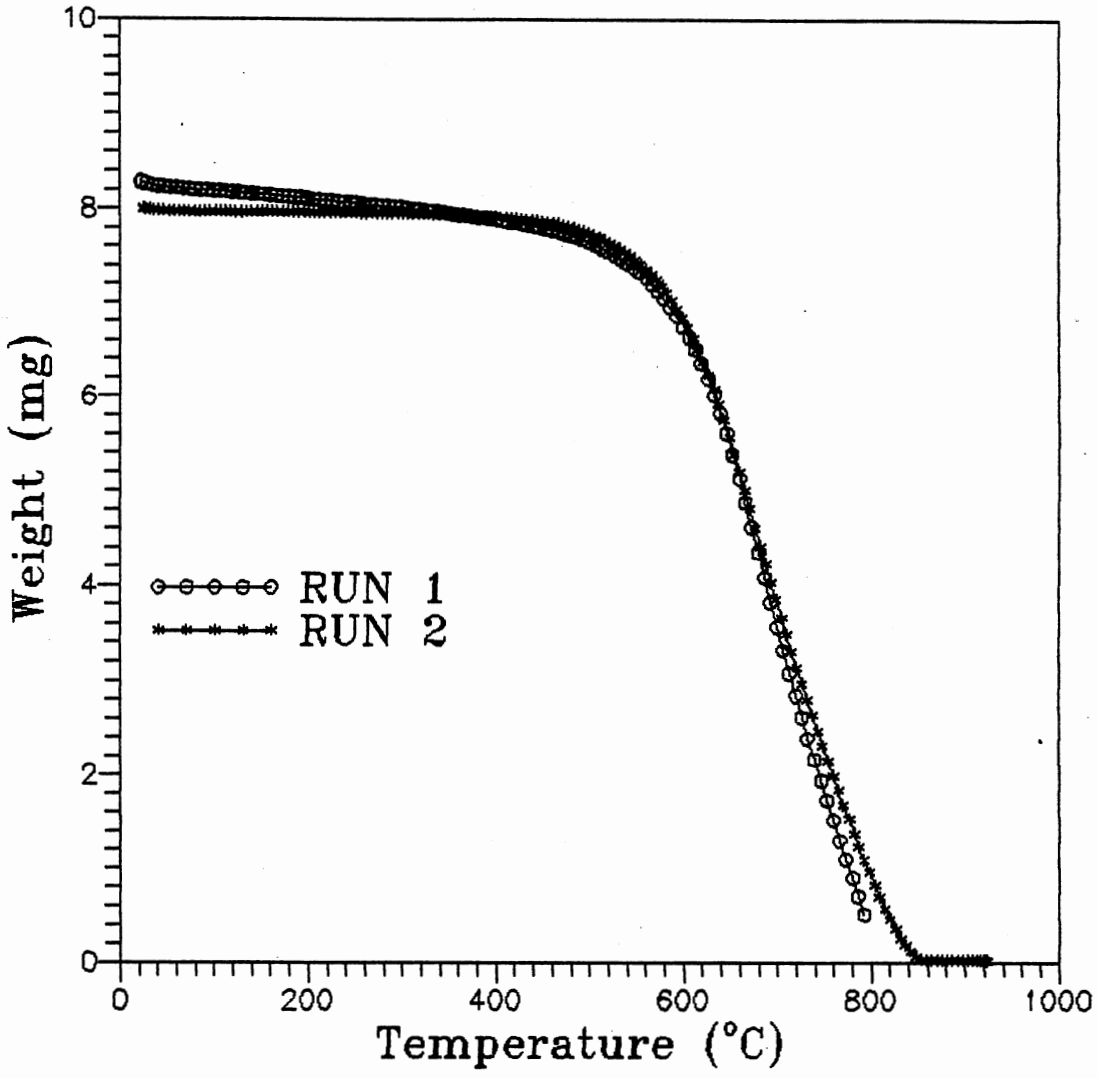

Figure 30. TGA Curves of Emeraldine Base at a Constant Heatin RAte 10°C/min

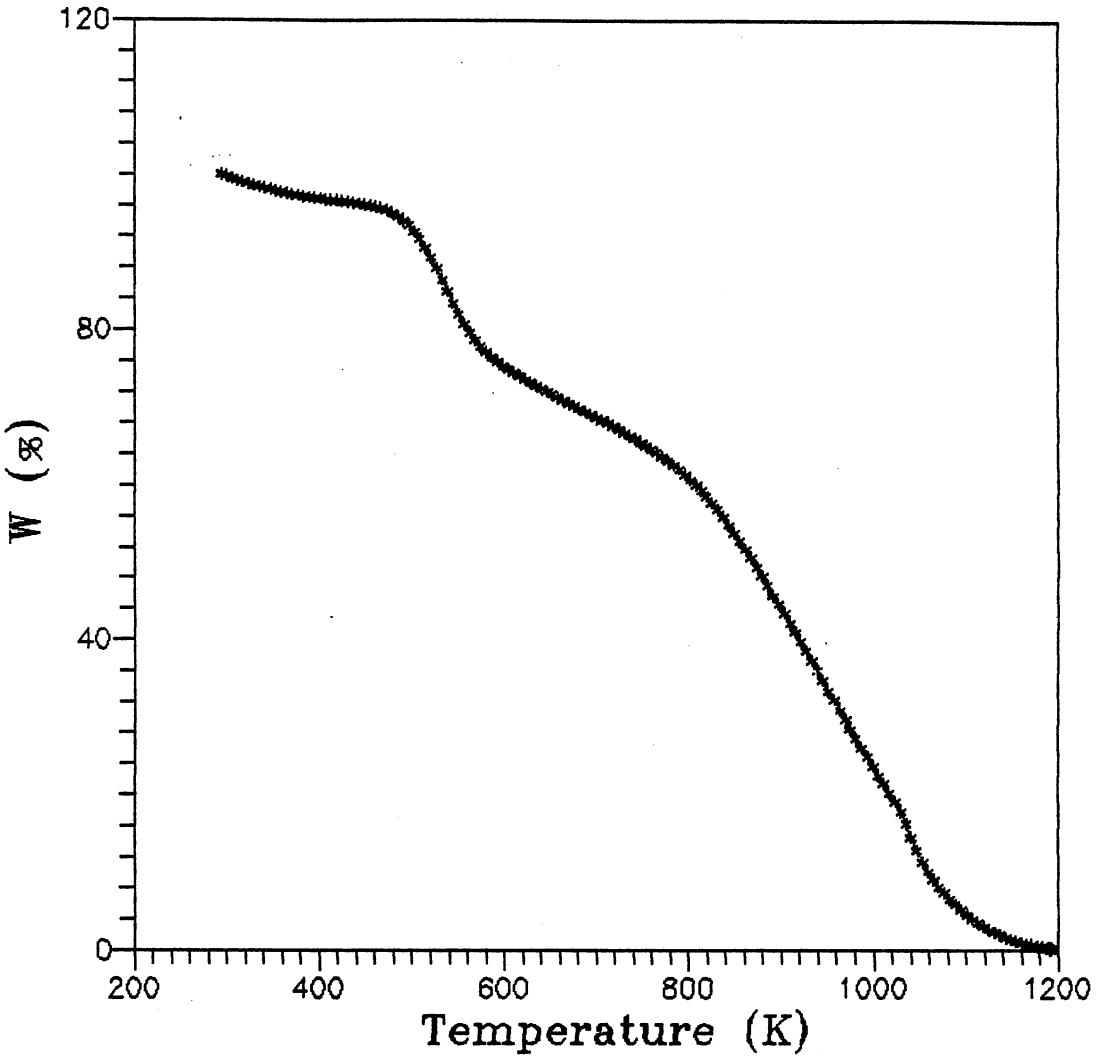

Figure 31. TGA Curve of Sulfonated Emeraldine at a Constant Heating Rate 3°C/min

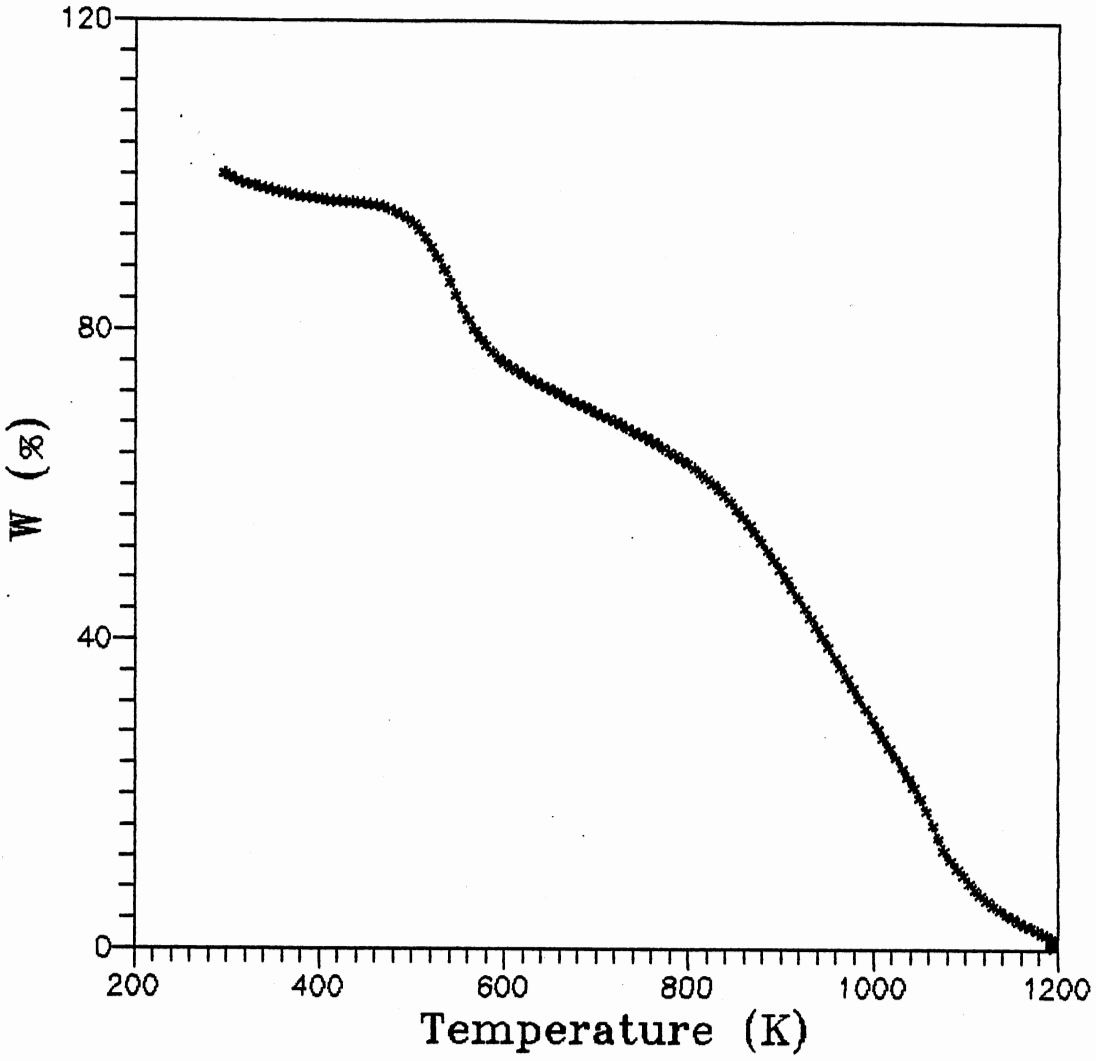

Figure 32. TGA Curve of Sulfonated Emeraldine at a Constant Heating Rate 5°C/min

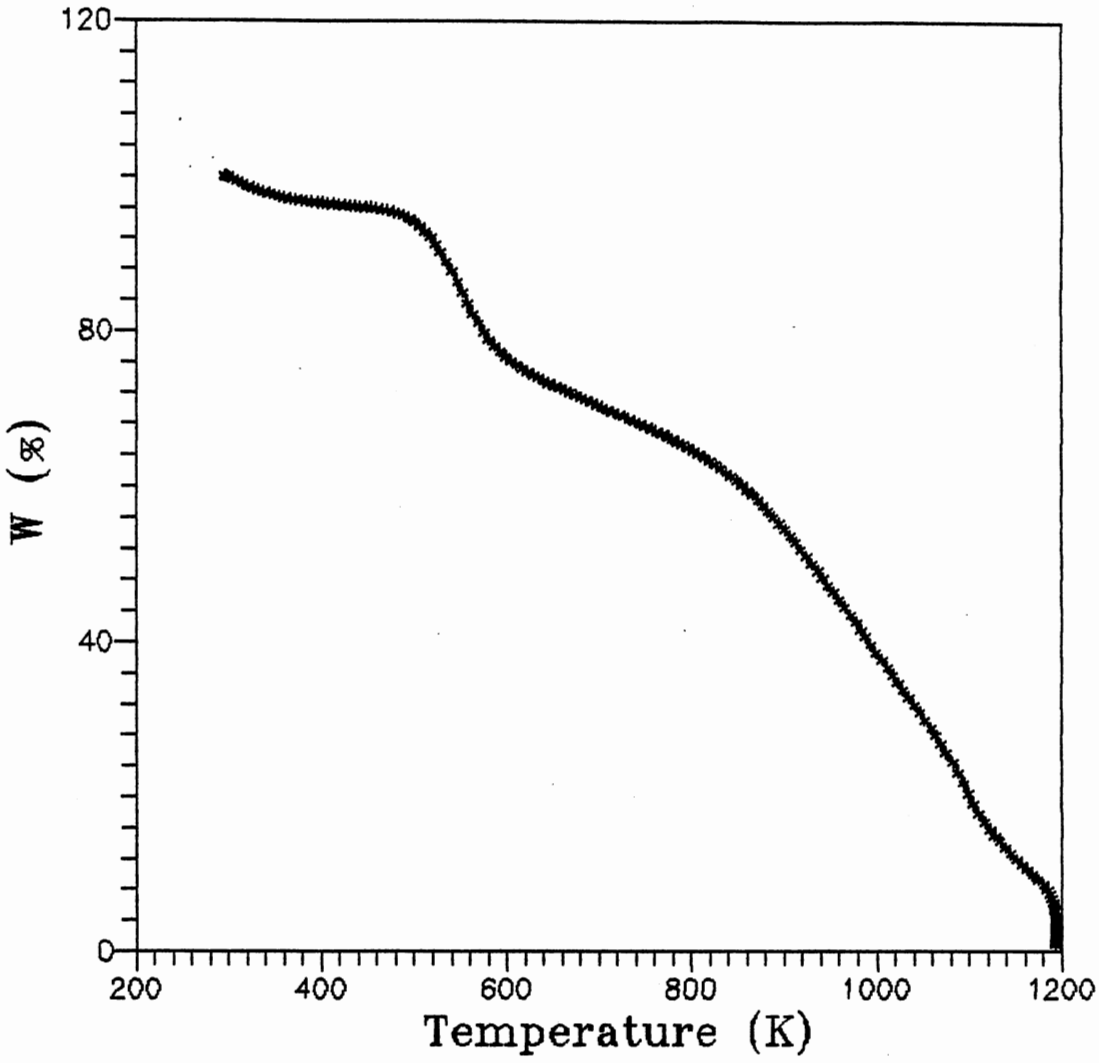

Figure 33. TGA Curve of Sulfonated Emeraldine at a Constant Heating Rate 10°C/min

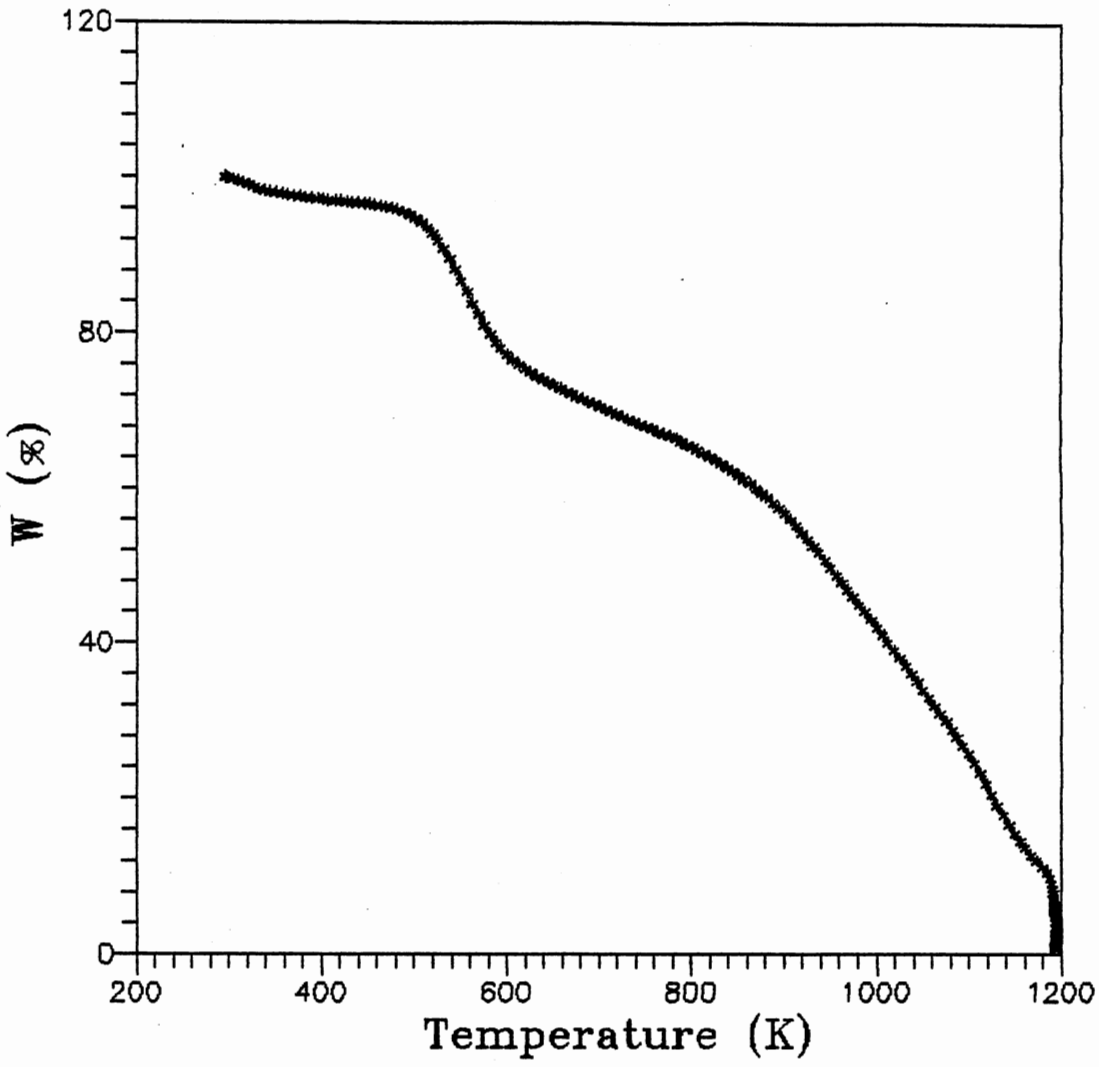

Figure 34. TGA Curve of Sulfonated Emeraldine at a Constant Heating Rate 15°C/min

APPENDIX B

DISCUSSION OF HIGHER REACTION ORDERS

From collision theory, reactions involving bimolecular collision are common, but collisions involving three molecules are rare, and greater than four are almost impossible. However, the reaction order can still be greater than 2 in many reactions. Following is the derivation of two reactions which behave like a third and forth order reaction, respectively.

Third Order Reaction

$$A + A \underset{k_2}{\overset{k_1}{\rightleftharpoons}} B$$

$$A + B \underset{k_4}{\overset{k_3}{\rightleftharpoons}} C$$

$$3\,A \rightleftharpoons C$$

$$r_A = -k_1 C_A^2 + k_2 C_B - k_3 C_A C_B + k_4 C_C$$

$$r_B = k_1 C_A^2 - k_2 C_B - k_3 C_A C_B + k_4 C_C$$

$$r_C = k_3 C_A C_B - k_4 C_C$$

where r_A: rate of reaction of component A

C_A: concentration of component A

Steady-state approximation, $r_B = 0$

$$C_B = \frac{k_1 C_A^2 + k_4 C_C}{k_2 + k_3 C_A}$$

substitution of C_B into r_A gives

$$r_A = -k_1 C_A^2 + \frac{k_1 k_2 C_A^2 - k_1 k_3 C_A^3 + k_2 k_4 C_C C_A - k_3 k_4 C_A C_C}{k_2 + k_3 C_A} + k_4 C_C$$

When $k_2 >> k_3$, we may approximate r_A as

$$r_A = -\frac{k_3 k_1 C_A^3}{K_2} - \frac{k_3 k_4 C_A C_C}{K_2} + k_4 (C_A + C_C)$$

The reaction order of concentration of component of A is third.

Fourth Order Reaction

$$A + A \underset{k_2}{\overset{k_1}{\rightleftharpoons}} B$$

$$A + B \underset{k_4}{\overset{k_3}{\rightleftharpoons}} C$$

$$A + C \underset{k_6}{\overset{k_5}{\rightleftharpoons}} D$$

$$4\,A \rightleftharpoons D$$

$$r_A = -k_1 C_A^2 + k_2 C_B - k_3 C_A C_B + k_4 C_C - k_5 C_A C_C + k_6 C_D$$

$$r_B = k_1 C_A^2 - k_2 C_B - k_3 C_A C_B + k_4 C_C$$

$$r_C = k_3 C_A C_B - k_4 C_C - k_5 C_A C_C + k_6 C_D$$

$$r_D = k_5 C_A C_C - k_6 C_D$$

Steady-state approximation, $r_B = 0$, and $r_C = 0$

$$C_B = \frac{k_1 k_4 C_A^2 + k_1 k_5 C_A^3 + k_4 k_6 C_D}{k_2 k_4 + k_2 k_5 C_A + k_3 k_5 C_A^2}$$

$$C_C = \frac{k_1 k_3 C_A^3 + k_2 k_6 C_D + k_3 k_6 C_A C_D}{k_2 k_4 + k_2 k_5 C_A + k_3 k_5 C_A^2}$$

Substitution of C_B, and C_C into r_A gives

$$r_A = k_6 C_D - \frac{k_1 k_3 k_5 C_A^4 + k_2 k_5 k_6 C_A C_D + k_3 k_5 k_6 C_A C_D}{k_2 k_4 + k_2 k_5 C_A + k_3 k_5 C_A^2}$$

APPENDIX C

COMPUTER PROGRAM

NOMENCLATURE FOR COMPUTER CODE

A: Pre-exponential factor; $min.^{-1}$

BETA: Heating rate; °C /min.; a

E: Activation energy; cal/mole

FIL1: File name of input data

FIL2: File name of output data

N: The reaction order

ND: Number of data would generate

T: Temperature; K

TI: Initial heating temperature; °C; T_0

TE: End heating temperature; °C

TT: Intergral term; $\int_{T_o}^{T} \exp(\frac{-\Delta E}{RT})\, dT$

WI: Initial weight percent at temperature T_0; W_0

WE: End weight percent at temperature TE; W

WP: Residue weight percent at temperature T

```
C   THIS PROGRAM WAS WRITTEN FOR CALCULATING THE WEIGHT LOSS
C        VERSUS TEMPERATURE CURVE.
C WRITTEN BY TSUNG-CHIEH TSAI
C APRIL 4 '92
C*************************************************************
C  TI : INITIAL TEMPERATURE (DEG C)
C  TE : END TEMPERATURE     (DEG C)
C  WI : INITIAL WEIGHT %
C  WE : END WEIGHT %
C  E  : ACTIVATION ENERGY   (cal/mole)
C  A  : PRE-EXPONENTIAL FACTOR
C  N  : THE ORDER OF REACTION (0,1,2,3,4)
C  ND : NUMBER OF DATA
C  BETA: HEATING RATE         ( DEG C/min)
C  TT : TEMPERATURE TERM  INTEGRAL FROM TI to T (EXP(-E/RT))
C
C*************************************************************
C
        IMPLICIT REAL*8 (A-H,O-Z)
        REAL*8 INTL
        REAL T,DELX,E
        CHARACTER*30 FIL1,FIL2
C---------------------------------------
C    DEFINE INPUT AND OUTPUT FILE NAME
C---------------------------------------
        WRITE(6,111)
111     FORMAT(/,'  ENTER INPUT FILE NAME, SUCH AS IN.PUT')
        READ(6,112) FIL1
112     FORMAT(30A)
        WRITE(6,113)
113     FORMAT(/,'  ENTER OUTPUT FILE NAME')
        READ(6,112) FIL2
        OPEN(UNIT=7,FILE=FIL1,STATUS='OLD')
        OPEN(UNIT=8,FILE=FIL2,STATUS='UNKNOWN')
        READ(7,*)TI,TE,WI,WE,E,A,N,ND,BETA
        TI=TI+273.15
        TE=TE+273.15
        DELX=(TE-TI)/ND
        N=N+1
        WRITE(8,150)
150     FORMAT('      TEMPERATRE          WEIGHT %')
        W=0.
        TT=0.
        T=TI
        GOTO(100,200,300,400,500) N
C**********************
C     0 ORDER
C**********************
100     DO 110 I=1,ND
        TT=TT+INTL(T,DELX,E)
        W=1.-A/BETA*TT
        WP=(W*(WI-WE)+WE)*100.
        WRITE(8,155)T,WP
110     T=T+DELX
        GOTO 600
```

```
C**********************
C   1ST ORDER
C**********************
200     DO 210 I=1,ND
        TT=TT+INTL(T,DELX,E)
        W=1.*EXP(-A/BETA*TT)
        WP=(W*(WI-WE)+WE)*100.
        WRITE(8,155)T,WP
210     T=T+DELX
        GOTO 600
C**********************
C   2ND ORDER
C**********************
300     DO 310 I=1,ND
        TT=TT+INTL(T,DELX,E)
        W=1./(1.+A/BETA*TT)
        WP=(W*(WI-WE)+WE)*100.
        WRITE(8,155)T,WP
310     T=T+DELX
        GOTO 600
C**********************
C   3RD ORDER
C**********************
400     DO 410 I=1,ND
        TT=TT+INTL(T,DELX,E)
        W=1./SQRT(1.+A/BETA/2.*TT)
        WP=(W*(WI-WE)+WE)*100.
        WRITE(8,155)T,WP
410     T=T+DELX
        GOTO 600
C**********************
C   4TH ORDER
C**********************
500     DO 510 I=1,ND
        TT=TT+INTL(T,DELX,E)
        W=(1./(1.+A/BETA/3.*TT)**(1./3.))
        WP=(W*(WI-WE)+WE)*100.
        WRITE(8,155)T,WP
510     T=T+DELX
        GOTO 600
155     FORMAT(4X,F12.3,4X,F12.3)
        CONTINUE
        CLOSE(7)
        CLOSE(8)
600     STOP
        END

        FUNCTION F(T,E)
        F=EXP(-E/1.987/T)
        RETURN
        END

C-------------------------------------------------------------

C CALCULATION OF THE INTEGRAL OF TEMPERATURE TERM BY SIMPSON'S
```

```
C-------------------------------------------------------------

      REAL*8 FUNCTION INTL(T,DELX,E)
      DELXS=DELX/16.
      INTL=0.
      T0=T
      DO 10 I=1,8
      T1=T0
      T2=T1+DELXS
      T3=T2+DELXS
      Y=DELXS/3.*(F(T1,E)+4*F(T2,E)+F(T3,E))
      INTL=INTL+Y
      T0=T3
10    CONTINUE
      RETURN
      END
```

```
C   THIS PROGRAM WAS WRITTEN FOR CALCULATING THE TEMPERATURE
C TERM.
C
C WRITTEN BY TSUNG-CHIEH TSAI
C NOV 12 '91
C FILENAME: INTLT.FOR
C*************************************************************
C
C  TI : INITIAL TEMPERATURE (DEG C)
C  TE : END TEMPERATURE     (DEG C)
C  E  : ACTIVATION ENERGY   (CAL /MOLE)
C  ND : NUMBER OF DATA
C  TT : TEMPERATURE TERM  INTEGRAL FROM TI to T (EXP(-E/RT))
C  ET : E/RT
C  TD : P(E/RT)  FROM Doyle
C
C*************************************************************
C
      REAL INTL
      CHARACTER*30 FIL1,FIL2
C-------------------------------------
C    DEFINE INPUT AND OUTPUT FILE NAME
C-------------------------------------
      WRITE(6,111)
111   FORMAT(/,'  ENTER INPUT FILE NAME, SUCH AS IN.PUT')
      READ(6,112) FIL1
112   FORMAT(30A)
      WRITE(6,113)
113   FORMAT(/,'  ENTER OUTPUT FILE NAME')
      READ(6,112) FIL2
      OPEN(UNIT=7,FILE=FIL1,STATUS='OLD')
      OPEN(UNIT=8,FILE=FIL2,STATUS='UNKNOWN')
      READ(7,*)TI,TE,WI,E,A,N,ND,BETA
      TI=TI+273.15
      TE=TE+273.15
      DELX=(TE-TI)/ND
      N=N+1
      WRITE(8,150)
150   FORMAT('      TEMPERATRE          WEIGHT')
      W=0.
      TT=0.
      T=TI
      DO 110 I=1,ND
      ET=E/1.987/T
      TT=TT+INTL(T,DELX,E)
      TD=TT/E*1.987
      WRITE(8,*)ET,TD
110   T=T+DELX
      CLOSE(7)
      CLOSE(8)
      STOP
      END

      FUNCTION F(T,E)
      F=EXP(-E/1.987/T)
```

```
      RETURN
      END

C-------------------------------------------------------------
C CALCULATINT THE INTEGRAL OF TEMPERATURE TERM BY SIMPSON'S
C-------------------------------------------------------------

      REAL FUNCTION INTL(T,DELX,E)
      DELXS=DELX/8.
      INTL=0.
      DO 10 I=1,4
      T1=T
      T2=T1+DELXS
      T3=T2+DELXS
      Y=DELXS/3.*(F(T1,E)+4*F(T2,E)+F(T3,E))
      INTL=INTL+Y
10    CONTINUE
      RETURN
      END
```

APPENDIX D

DSC DATA

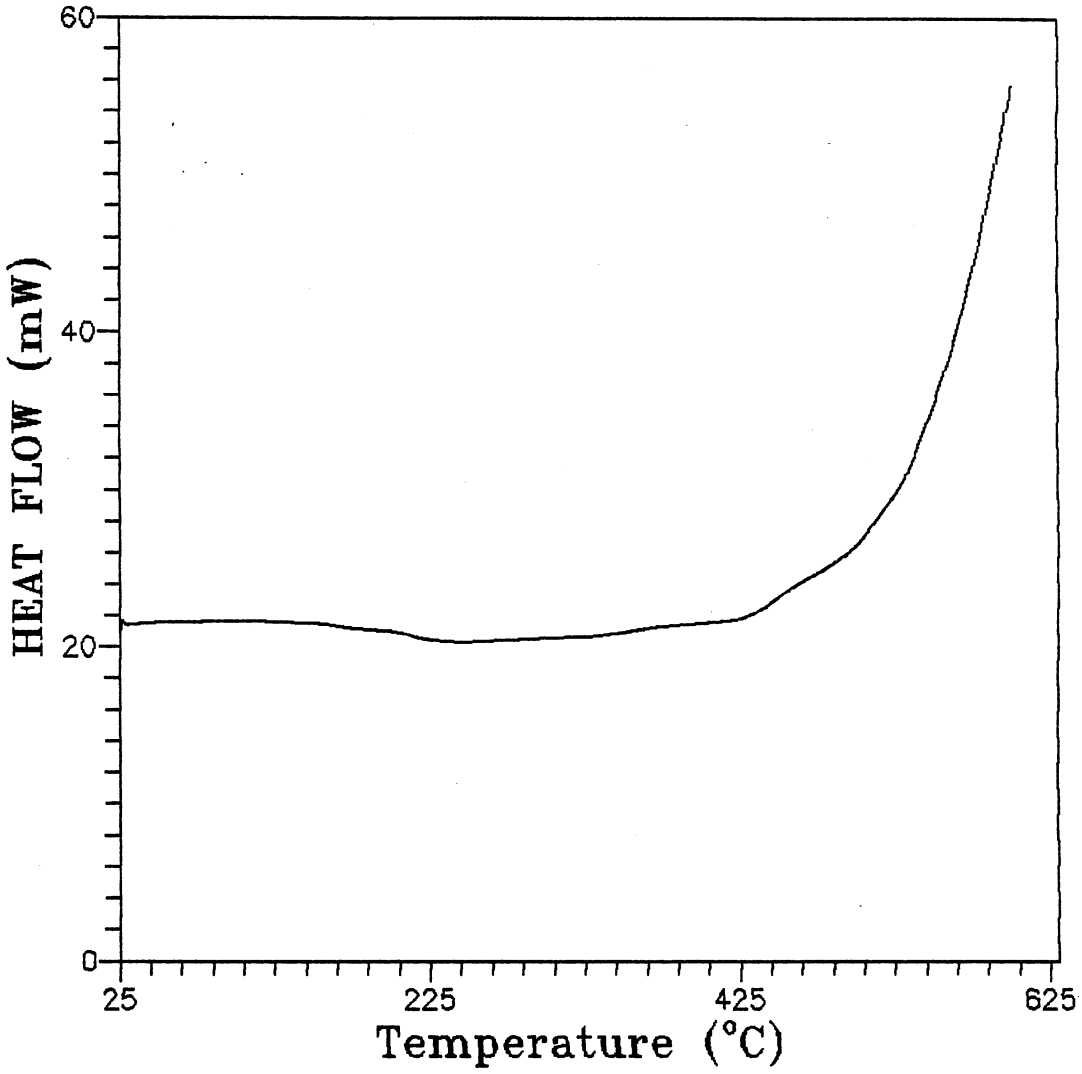

Figure 35. DSC Curve of Emeraldine Base at Scanning Rate 10°C/min in Nitrogen Environment

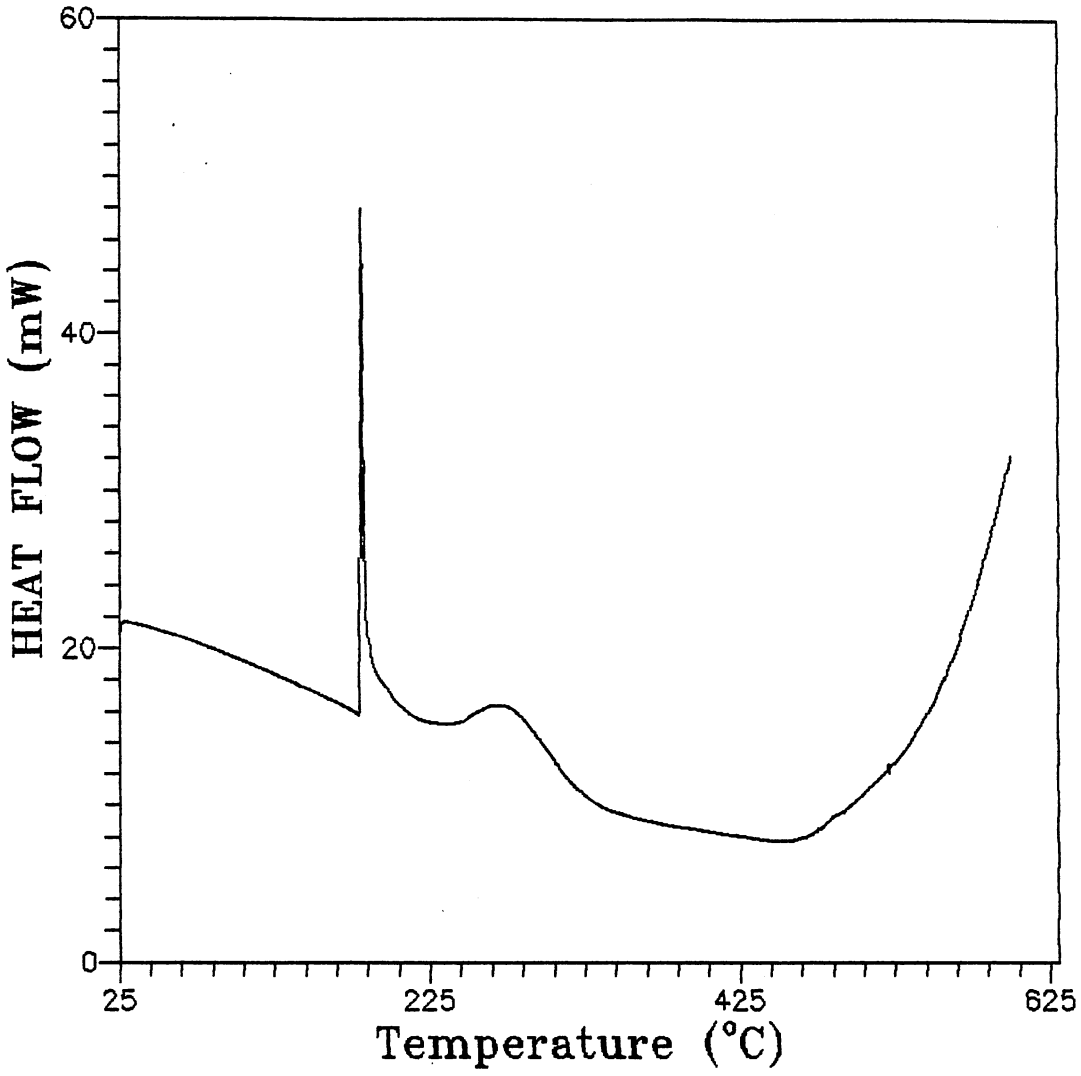

Figure 36. DSC Curve of Sulfonated Emeraldine at Scanning Rate 10°C/min in Nitrogen Environment

APPENDIX E

SAMPLES OF GAS CHROMATOGRAM

From the procedure mentioned in Chapter 3, the gas chromatography peaks should appear in the order depicted in Figure 37, beginning with Hydrogen followed by carbon dioxide, acetylene, etc.; and at the retention time shown in Table V. Care should be take to identify the peaks due to valve switching. These peaks occurred at 0 min, 2.75 min and 5.0 min respectively and may be a positive or negative deflection in the chromatogram. There may also be two or more peaks caused by the valve switching. Valve switching peaks may be identified with certainty since they will appear in every chromatogram regardless of the composition of the sample. The following chromatograms were taken before the degradation began (Figure 38), at 716°C (Figure 39), and 20 min after temperature reached 925°C (Figure 40), respectively.

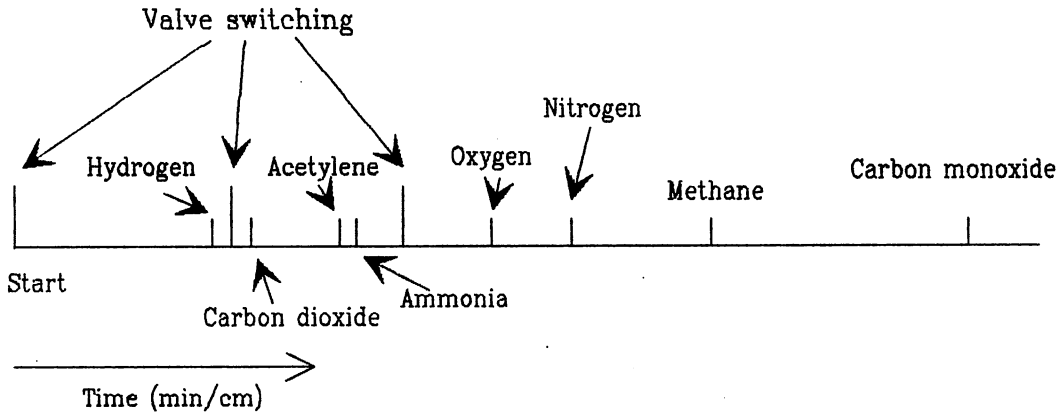

Figure 37. Gas Chromatogram Peaks Order of Appearance

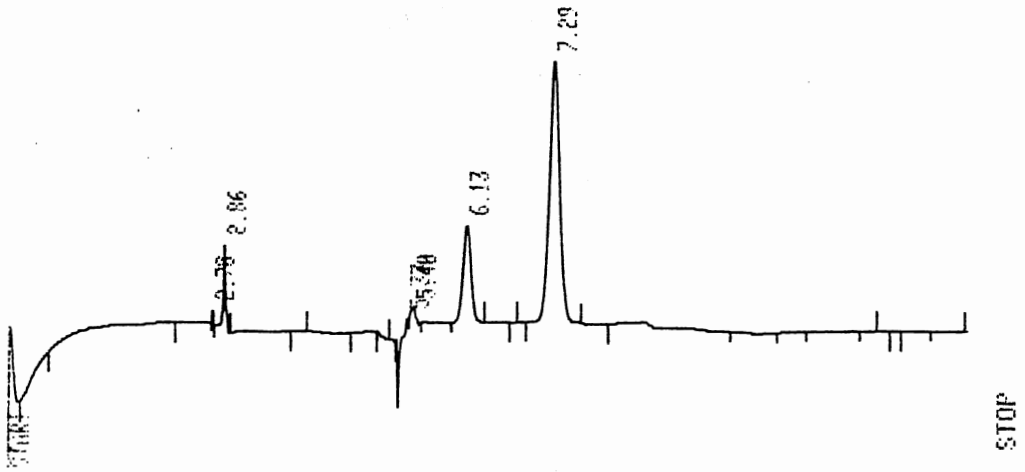

Figure 38. Gas Chromatogram Taken Before Degradation Began

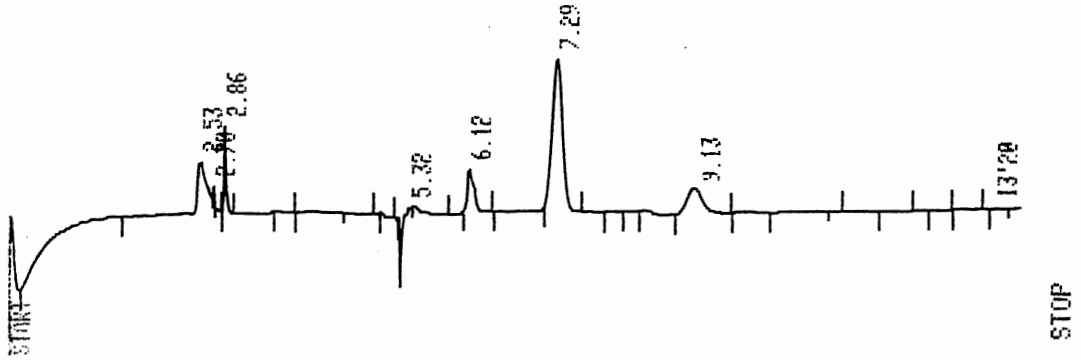

Figure 39. Gas Chromatogram Taken at 716°C

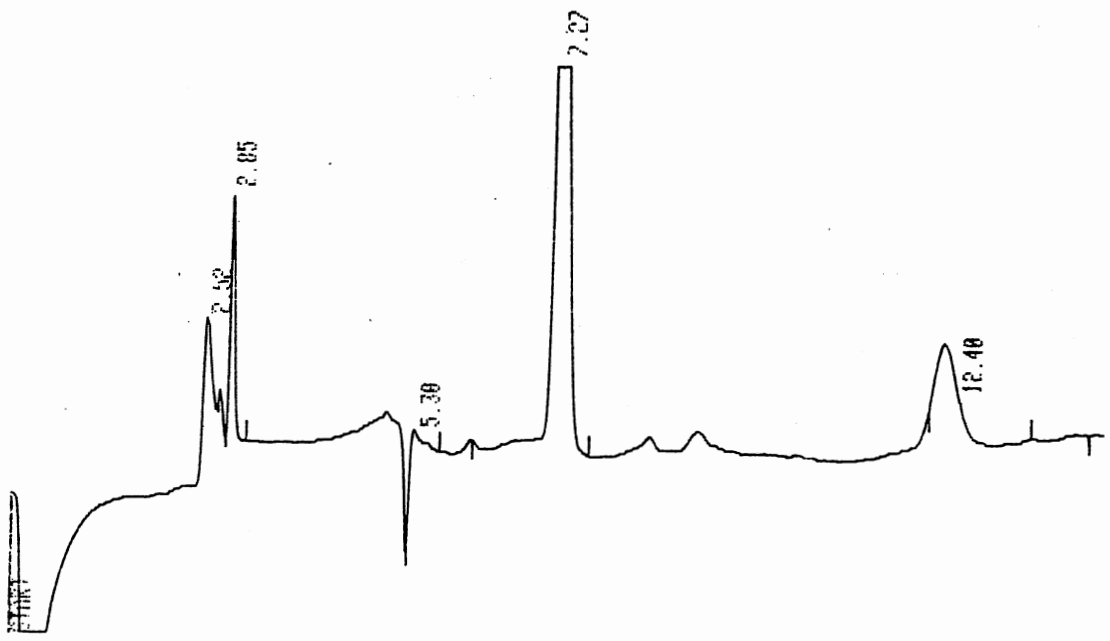

Figure 40. Gas Chromatogram Take 20 min After Temperature Reached 925°C

Referring to Figure 38, the first negative peak is due to the first switch and occurred time = 0.2 min. The peaks labeled 2.78 min and 2.86 min were due to the second switch. The peaks labeled 5.37 min and 5.40 min are due to the third switch. Note that the third switch resulted in a negative and two positive deflections. The remaining peaks at 6.13 min and 7.29 min are due to oxygen and nitrogen, respectively. Corresponding peaks are readily identified in Figures 39 and 40. The additional small peak in Figure 40 at 8.4 min was ignored due to the fact that a corresponding peak occurred in Figure 38 at a temperature (21°C) at which no degradation could have occurred.

VITA

Tsung-chieh Tsai

Candidate for the Degree of

Master of Science

Thesis: THE THERMODEGRADATION AND THE DEGRADATION PRODUCTS OF POLYANILINE

Major Field: Chemical Engineering

Biographical:

Personal Data: Born in Tainan, Taiwan, August 27, 1964, the son of Chao-chan Tsai and Chin-ying Tsai-Hu.

Education: Graduated from Kung Shan Institute of Technology, Tainan, Taiwan in June 1984; received Bachelor of Science Degree in Chemical Engineering from National Institute of Technology at Taipei in June, 1989; completed requirements for the Master of Science degree at Oklahoma State University in July, 1992.

Personal Experience: Maintenance Engineer, Jang-Dah Nylon Inc.,Process control engineer, Department of Computer & Control Engineering, Advance Control & Systems Inc., October, 1989, to July, 1990.Teaching Assistant, School of Chemical Engineering, Oklahoma State University, August, 1990, to May, 1991. Research Assistant, School of Chemical Engineering, Oklahoma State University, August, 1991, to December, 1991.